Contract No:

This document was prepared in conjunction with work accomplished under Contract No. DE-AC09-08SR22470 with the U.S. Department of Energy (DOE) Office of Environmental Management (EM).

Disclaimer:

This work was prepared under an agreement with and funded by the U.S. Government. Neither the U. S. Government or its employees, nor any of its contractors, subcontractors or their employees, makes any express or implied:

1) warranty or assumes any legal liability for the accuracy, completeness, or for the use or results of such use of any information, product, or process disclosed; or
2) representation that such use or results of such use would not infringe privately owned rights; or
3) endorsement or recommendation of any specifically identified commercial product, process, or service.

Any views and opinions of authors expressed in this work do not necessarily state or reflect those of the United States Government, or its contractors, or subcontractors.

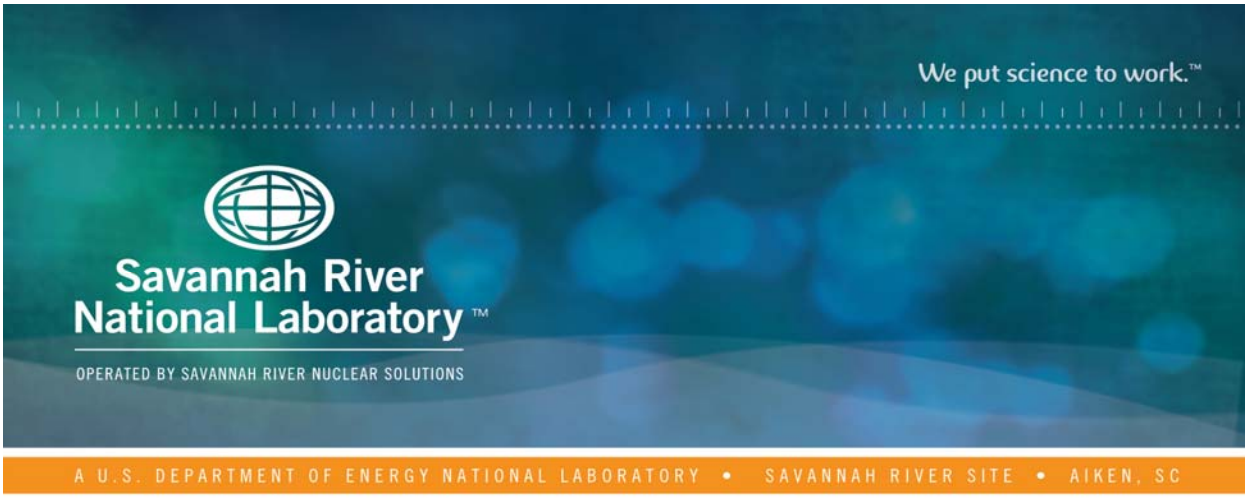

Results for Actinide Removal Process 512-S Guard Filter Analyses

C. J. Bannochie

M. L. Restivo

T. B. Peters

February 2015

SRNL-STI-2014-00518, Revision 0

DISCLAIMER

This work was prepared under an agreement with and funded by the U.S. Government. Neither the U.S. Government or its employees, nor any of its contractors, subcontractors or their employees, makes any express or implied:

1. warranty or assumes any legal liability for the accuracy, completeness, or for the use or results of such use of any information, product, or process disclosed; or
2. representation that such use or results of such use would not infringe privately owned rights; or
3. endorsement or recommendation of any specifically identified commercial product, process, or service.

Any views and opinions of authors expressed in this work do not necessarily state or reflect those of the United States Government, or its contractors, or subcontractors.

Printed in the United States of America

Prepared for
U.S. Department of Energy

SRNL-STI-2014-00518
Revision 0

Keywords: *MCU, ARP, ISDP*

Retention: *Permanent*

Results for Actinide Removal Process 512-S Guard Filter Analyses

C. J. Bannochie
M. L. Restivo
T. B. Peters

February 2015

Prepared for the U.S. Department of Energy under contract number DE-AC09-08SR22470.

Savannah River National Laboratory™
OPERATED BY SAVANNAH RIVER NUCLEAR SOLUTIONS

REVIEWS AND APPROVALS

AUTHORS:

C. J. Bannochie, Process Technology Programs Date

M. L. Restivo, Advanced Characterization & Processing Date

T. B. Peters, Advanced Characterization & Processing Date

TECHNICAL REVIEW:

C. J. Martino, Advanced Characterization & Processing, Reviewed per E7 2.60 Date

APPROVAL:

F. M. Pennebaker, Manager Date
Advanced Characterization & Processing

S.L. Marra, Manager Date
Environmental & Chemical Process Technology Research Programs

E. J. Freed, Manager Date
DWPF/Saltstone Facility Engineering

PREFACE OR ACKNOWLEDGEMENTS

The authors wish to thank SRNL Shielded Cells personnel Kevin Reid, Nan Stanley, and Ron Blessing for their expertise in sectioning the 512-S filter tubes and preparing samples for submission to Analytical Development (AD). We thank all AD personnel for the analyses performed, but especially Dr. Henry Ajo for the extensive work he conducted acquiring the scanning electron microscopy (SEM) images and energy dispersive spectroscopy (EDS) spectra, and David Missimer for his responsiveness in conducting the x-ray fluorescence (XRF) and x-ray diffraction (XRD) analyses. We also thank Dr. Fernando Fondeur for FTIR analyses and interpretation, and Dave Herman for contributions to filter and process history in 512-S.

EXECUTIVE SUMMARY

The Actinide Removal Process (ARP) removes Sr and actinides by adsorption to monosodium titanate (MST) from radioactive salt solutions that have been stored at the Savannah River Site (SRS). The MST solids are then removed by filtration. Material from the 512-S Late Wash Precipitate Tank (LWPT) is cross-flow filtered and the filtrate sent through a secondary filter (guard filter) to the Late Wash Hold Tank (LWHT) for further processing in the Modular Caustic Side Solvent Extraction (CSSX) Unit (MCU). This process flow diagram is shown below.

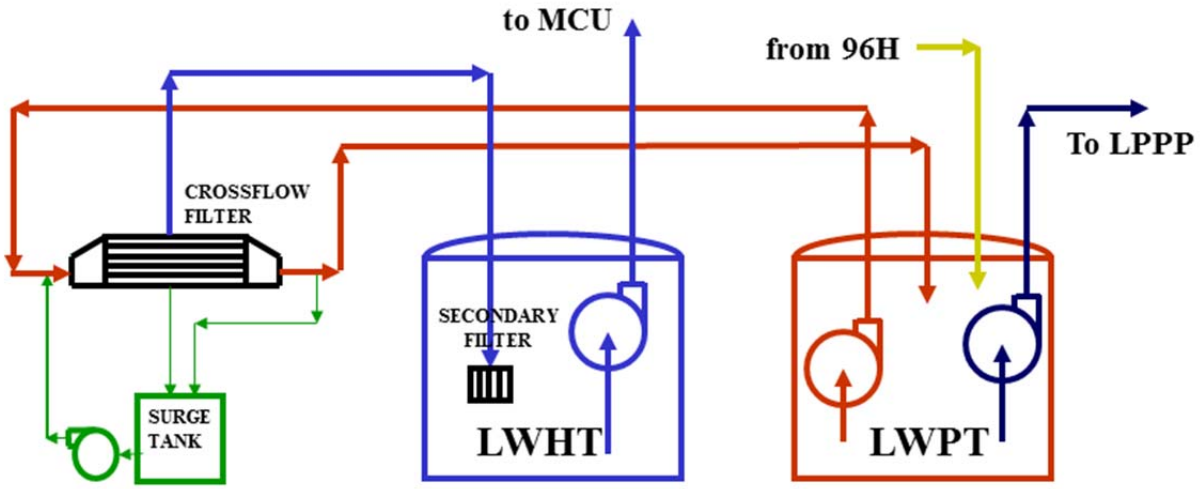

Simplified diagram of the 512-S portion of ARP

The 512-S Facility process used a nominal 0.1 µm Mott filter bundle until February 2014 to separate monosodium titanate (MST) solids from dissolved salt and supernatant liquid. The 512-S Facility has processed over 4 Mgal of supernatant and dissolved salt with the original 0.1 µm Mott filter. After approximately seven years in service, the 0.1 µm filter was replaced with a 0.5 µm Mott filter bundle. The original crossflow filter (CFF) unit in the 512-S Facility contained 144 Mott sintered metal filter tube elements and a total filter area of 230 ft^2. The replacement 0.5 µm filter is of similar size (dimensional) and construction, with the only difference in the filter being porosity (0.5 versus 0.1 µm). The filter tubes are made of 316 stainless steel, with an inner diameter of 0.625 in. and a length of 120 in.

The secondary filter is downstream of the CFF. The secondary filter is a dead-end filter constructed of 21 sintered metal filter tubes with a 0.5 µm nominal rating, with a total surface area of 16.5 ft^2. The tubes are made from 316 stainless steel and are also manufactured by Mott®. The filter elements sit inside the LWHT.

In order to optimize the performance of salt processing by increasing material throughput, it is necessary to address a significant pressure drop across the guard or secondary filter. The pressure drops have increased recently, and coincide with recent operational upset conditions occurring in the MCU. These upset conditions occurred in April and August 2014, initiating a desire to understand the chemistry related to the performance changes. The operational performance of the filter in ARP has historically been the limiting factor in salt processing. As a result, post-use analyses of the filtration media has been requested to ascertain the characteristics of the filter loading that may help determine upstream upset conditions or causes for the observed pressure drop. A Task Technical and Quality Assurance Plan (TTQAP) was written in response to this Technical Task Request (TTR).

ARP/MCU sent two spent filters from the 512-S facility to the Savannah River National Laboratory's (SRNL) Shielded Cells facility which were designated as follows:

- Filter 1 – the filter removed from service in the August 2014 timeframe.
- Filter 2 – the filter removed from service in the April 2014 timeframe.

Filter 1 processed approximately 187,000 gallons of Tank 49 material composed of Salt Batch 7a (SaB7a). Filter 2 processed approximately, 487,000 gallons of Tank 49 material composed of Salt Batch 6d (SaB6d) and the first six batches of SaB7a. The primary filter was changed between the end of SaB6d and the start of SaB7a.

The 512-S secondary filters received by SRNL did not show major fouling upon visual examination. Closer inspection indicated evidence of aluminosilicates, aluminum hydroxides, silica, monosodium titanate (MST), and various sulfates and chlorides in addition to various salts of nitrates, nitrites, carbonates. Filter 2 contained Hg compounds, possibly elemental, that was not observed on Filter 1. Scanning electron microscopy (SEM) examination indicated more solids on Filter 1 than Filter 2, which is consistent with it having not been rinsed prior to delivery to SRNL. The solids that are present appear to be fines that made it through the primary filter and became lodged in the secondary filter. There is some evidence these fines are penetrating into the sintered metal surface and possibly working their way through the secondary filter. It may be these lodged fines that are resulting in the increased pressure drop across the secondary filter.

Comparing the current findings with the 2009 secondary filter analyzed in SRNL we find the following:

1. There was no $CO_{2(g)}$ generation observed during acid leaching of the coupons which is consistent with the lower amount of carbonate salt deposits observed on these filters.
2. MST was not observed on the current filters when examined by x-ray diffraction spectroscopy (XRD) as it was in 2009, and only a trace was found by Fourier transform infrared spectroscopy (FTIR), though the SEM - energy dispersive spectroscopy, x-ray fluorescence (XRF), and acid-leached coupons examined by ICP-AES indicate its presence (measured as Ti) on the filters.
3. Sr-90 is once again the largest contributor to the dose amongst the analyzed radionuclides, but it is difficult to compare activities with the 2009 filter since the earlier leach results were not expressed in units of filter area.
4. Oxalate was the least abundant anion measured while it was the most abundant in the 2009 study.
5. After Na (from salts) and Fe (leached from the stainless steel), Ti was the most abundant metal ion observed in the leachates, and once again its most likely source term is MST fines that made it through the primary filter.

If Hg is present on the primary filter, as it is expected to be since the filtrate from the primary filter is the source term for the Hg observed on the secondary Filter 2, oxalic acid cleaning may not be suitable. Both HgC_2O_4 and $Hg_2C_2O_4$ are considered insoluble in water and the Hg(I) oxalate is only slightly soluble in dilute nitric acid. Cleaning the filter with nitric acid may be the only option to remove deposited Hg.

The following recommendations for future work are made based upon items learned from this study:

1. Examine the primary filter now that we have examined three secondary filters to see if fines are also lodged in the filter media. This would include examining the primary filter for pockets of Hg.
2. Examine the filter performance of an entire filter tube from an existing secondary filter bundle to evaluate its performance and correlate this performance with the characterization data found for that filter.

3. Future filter examinations should look at larger pieces of filter than was done in this study where some pieces were as small as one quarter of a square inch. It is unclear what impact the intense localized heating created by the cutting tool had on these very small coupons as compared to larger coupons, but larger coupons would minimize this impact.
4. Leaching tests could be conducted on larger 3"L pieces of tube, while SEM could be conducted on 3"L tubes that were bisected into two halves and XRD/XRF measurements on halves that had been further size reduced by snapping rather than cutting.
5. To eliminate cross contamination, the Shielded Cells manipulator fingers and/or vice should be replaced prior to handling the samples, and kept clean between handling operations.

TABLE OF CONTENTS

LIST OF TABLES

LIST OF FIGURES

LIST OF ABBREVIATIONS

AD	Analytical Development
ARP	Actinide Removal Process
BSD	Backscattered Electron Detector
CFF	Crossflow Filter
CSSX	Caustic-Side Solvent Extraction
dpm	Disintegrations Per Minute
FTIR	Fourier Transform Infrared Spectroscopy
IC	Ion Chromatography
ICP-AES	Inductively Coupled Plasma – Atomic Emission Spectroscopy
LAW	Low-Activity Waste
LWHT	Late Wash Hold Tank
LWPT	Late Wash Precipitate Tank
MCU	Modular Caustic-Side Solvent Extraction Unit
Mgal	Million Gallons
MST	Monosodium Titanate
NAS	Sodium Aluminum Silicate
SaB1	Salt Batch 1
SaB6d	Salt Batch 6d
SaB7a	Salt Batch 7a
SaB7b	Salt Batch 7b
SE	Secondary Electron (Detector)
SRNL	Savannah River National Laboratory
SRS	Savannah River Site
SEM-EDS	Scanning Electron Microscopy – Energy Dispersive Spectroscopy
TICTOC	Total Inorganic Carbon / Total Organic Carbon
TTQAP	Task Technical and Quality Assurance Plan
TTR	Technical Task Request
WAC	Waste Acceptance Criteria
XRD	X-Ray Diffraction Spectroscopy
XRF	X-Ray Fluorescence Spectroscopy

1.0 Introduction

The Actinide Removal Process (ARP) removes Sr and actinides by adsorption to monosodium titanate (MST) from radioactive salt solutions that have been stored at the Savannah River Site (SRS). The MST solids are then removed by filtration. Material from the 512-S Late Wash Precipitate Tank (LWPT) is cross-flow filtered and the filtrate sent through a secondary filter (guard filter) to the Late Wash Hold Tank (LWHT) for further processing in the Modular Caustic Side Solvent Extraction (CSSX) Unit (MCU). This process flow diagram is shown in Figure 1-1.

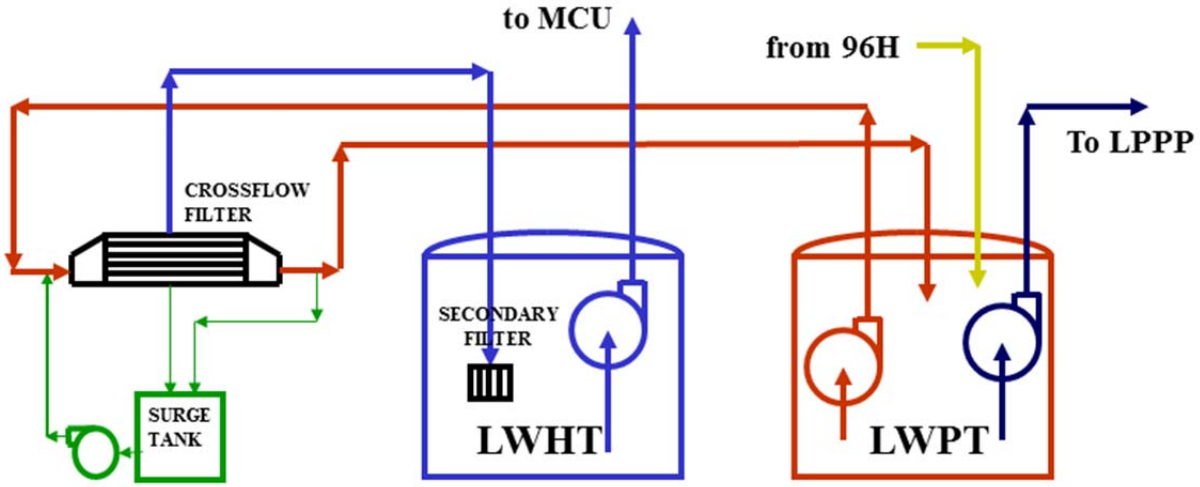

Figure 1-1 Simplified diagram of the 512-S portion of ARP

The 512-S Facility process used a 0.1 µm Mott filter bundle until February 2014 to separate monosodium titanate (MST) solids from dissolved salt and supernatant liquid. The 512-S Facility has processed over 4 Mgal of supernatant and dissolved salt with the original 0.1 µm Mott filter. After approximately seven years in service, the 0.1 µm filter was replaced with a 0.5 µm Mott filter bundle. The original crossflow filter (CFF) unit in the 512-S Facility contained 144 Mott sintered metal filter tube elements and a total filter area of 230 ft^2. The replacement 0.5 µm filter is of similar size (dimensional) and construction, with the only difference in the filter being porosity (0.5 versus 0.1 µm). The filter tubes are made of 316 stainless steel, with an inner diameter of 0.625 in. and a length of 120 in.

The secondary filter is downstream of the CFF. The secondary filter is a dead-end filter constructed of 21 sintered metal filter tubes with a 0.5 µm nominal rating, with a total surface area of 16.5 ft^2. The tubes are made from 316 stainless steel and are also manufactured by Mott®. The filter elements sit inside the LWHT.

In order to optimize the performance of salt processing by increasing material throughput, it is necessary to address a significant pressure drop across the guard or secondary filter. The pressure drops have increased recently, and coincide with recent operational upset conditions occurring in the MCU. These upset conditions occurred in April and August 2014, initiating a desire to understand the chemistry related to the performance changes. The operational performance of the filter in ARP has historically been the limiting factor in salt processing.[1] As a result, post-use analyses of the filtration media has been requested [2] to ascertain the characteristics of the filter loading that may help determine upstream upset

conditions or causes for the observed pressure drop. A Task Technical and Quality Assurance Plan (TTQAP) [3] was written in response to this Technical Task Request (TTR).[2]

ARP/MCU sent two spent filters (see Figure 1-2) from the 512-S facility to the Savannah River National Laboratory's (SRNL) Shielded Cells facility which were designated as follows:

- Filter 1 – the filter removed from service in the August 2014 timeframe.
- Filter 2 – the filter removed from service in the April 2014 timeframe.

Filter 1 processed approximately 187,000 gallons of Tank 49 material composed of Salt Batch 7a (SaB7a). Filter 2 processed approximately, 487,000 gallons of Tank 49 material composed of Salt Batch 6d (SaB6d) and the first six batches of SaB7a. The primary filter was changed between the end of SaB6d and the start of SaB7a. Prior to receipt by SRNL, Filter 2 was rinsed with water, while Filter 1 was not rinsed.

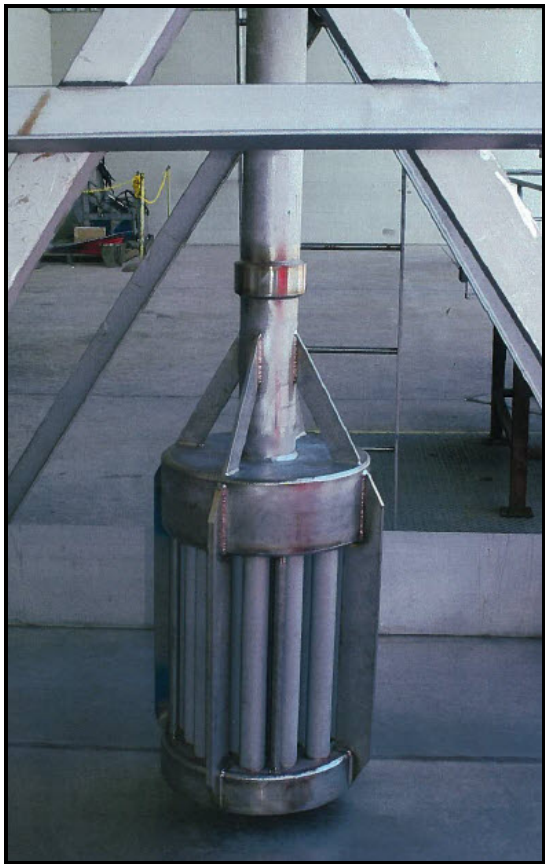

Figure 1-2 512-S Secondary Filter or Guard Filter

A more detailed timeline showing primary filter cleaning, secondary filter replacements, and processing conditions is shown in Figure 1-3 from information drawn from the OSIsoft PI System (v.3.2.0.0) displayed in the PI Process Book. Recent information reveals that 512-S performance degrades significantly following cross-flow filter cleaning. The cleaning operation results in an increased filtrate pressure and reduced throughput, but this increase in filtrate pressure diminishes after a period of operations, usually less than ten batches, suggesting that whatever is released from the primary filter eventually either dissolves or works it way through the secondary filter. It should be noted that the

August cross-flow filter cleaning was less routine in that the contents of the surge tank (Figure 1-1) were transferred to the LWPT prior to the start of cleaning. It is possible that the composition of the feed from the LWPT was changed prior to cleaning and washing.

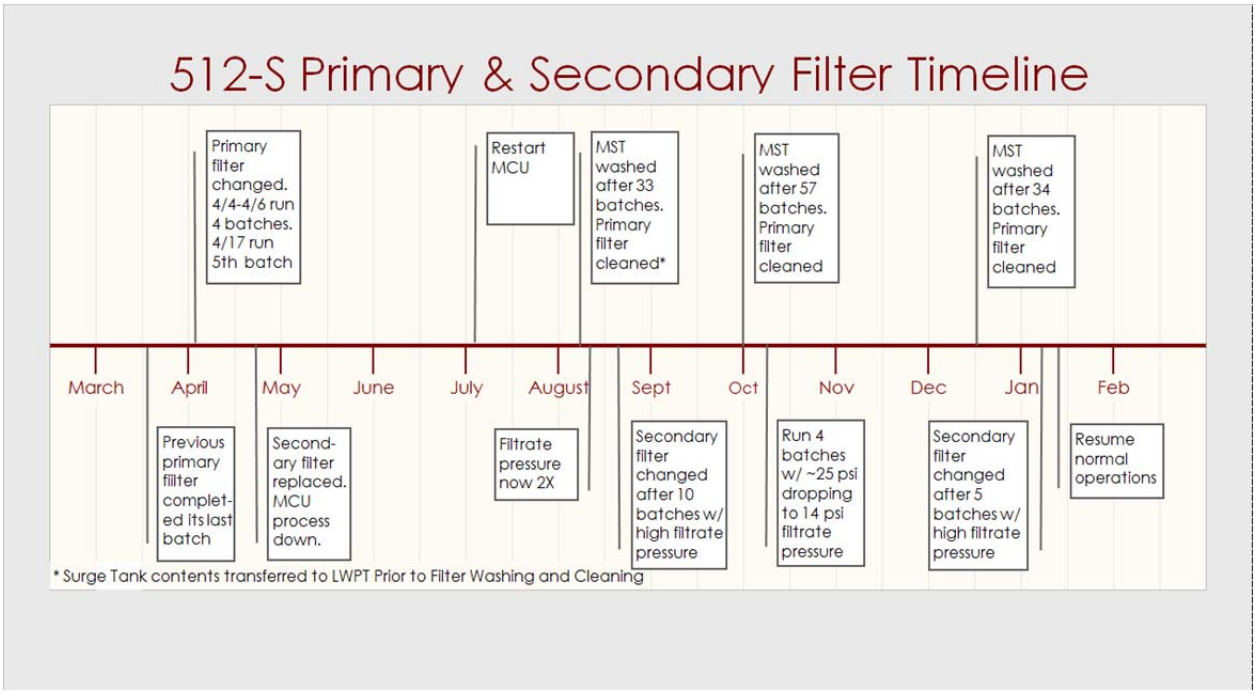

Figure 1-3 Timeline of 512-S Filter Operations between March 2014 and February 2015.

2.0 Experimental Procedure

2.1 Visual Inspection

Prior to cutting the assembly for Filter 1 coupon collection, a visual inspection of the inner tube surface was made starting at the four inch feed tube and continuing down into the filter tube array and individual filter tubes. Both still photographs and video were taken.[4,5] Representative images are shown in Figure 3-1, and will be discussed in Section 3.1. Filter 2 did not undergo a visual inspection prior to sample collection.

2.2 Filter Sampling

Each filter was sectioned by mechanical methods to remove coupons from the sintered metal filtration media using a Sonicrafter 2.5 Amp Oscillating Multi-Tool, which minimized spark concerns in the Shielded Cells facility. The sequence of coupon removal is displayed in Figure 2-1 and Figure 2-2. First the filter tube was cut vertically about one inch apart. Then a punch-out area was made at the top with two perpendicular cuts. Generally, the manipulator finger was used to bend back the coupon after it was cut free on three sides, but a screwdriver was used on some of the early coupons when the breakaway hole shown in the top, middle image of Figure 2-1 was too small for the manipulator finger. Once bent back, the coupon strip would snap off of the main filter tube. The three to four inch strip was then snapped into four individual coupons using a vice as shown in the last bottom image of Figure 2-1.

Thirty-two, roughly one square inch coupons (range: 0.25- 1.5 sq. inches) were created from each filter (four cutting locations per level, two levels, and four coupons per location). Coupon locations were selected to determine if vertical stratification and asymmetric loading had occurred. A diagram of the filter coupon locations is shown in Figure 2-3 and Figure 2-4 with our best estimates for vertical locations of where the coupons originated. The radial locations are firmly established and not estimated.

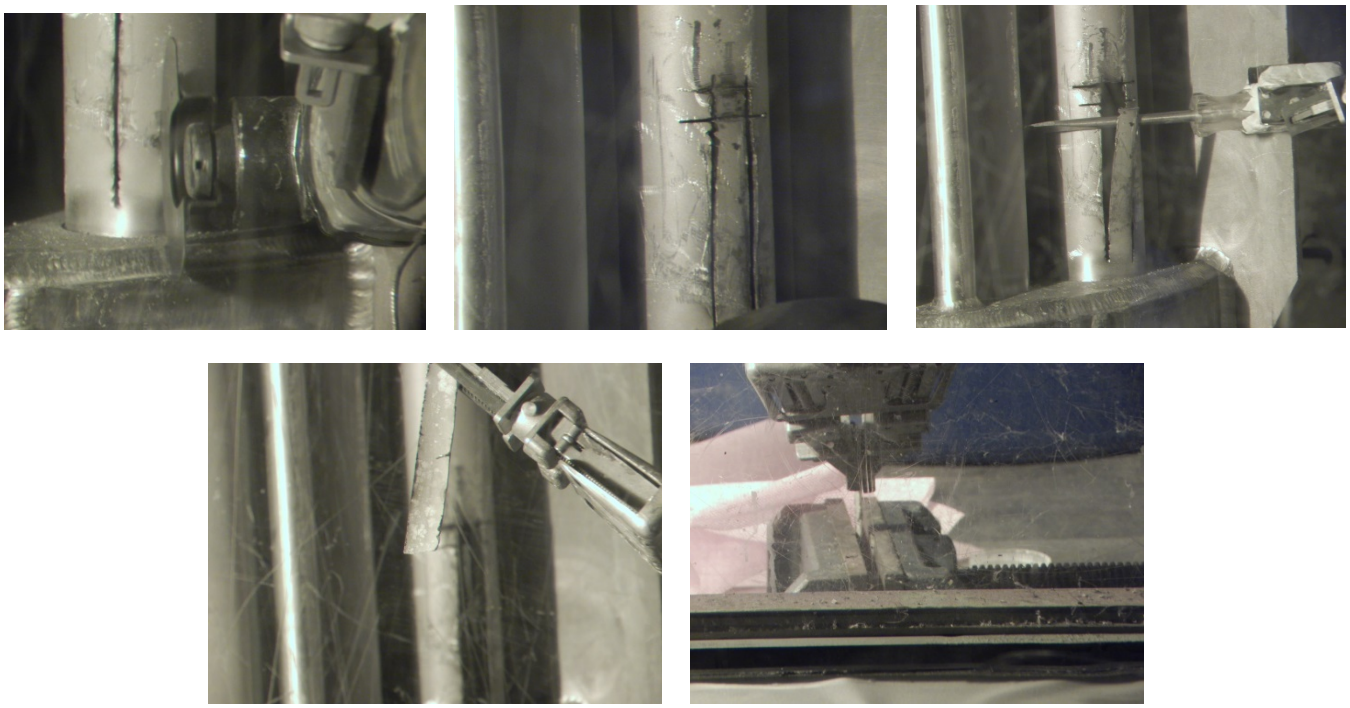

Figure 2-1 Shielded Cells Sampling Sequence for 512-S Filter 1 Coupon Collection. From left to right, then top to bottom: cutting, pop-out creation, coupon separation, coupon removal, and placement in vice for sub-sectioning.

Figure 2-2. Shielded Cells Sampling Sequence for 512-S Filter 2 Coupon Collection. From left to right: cutting, pulling, and removal of a coupon.

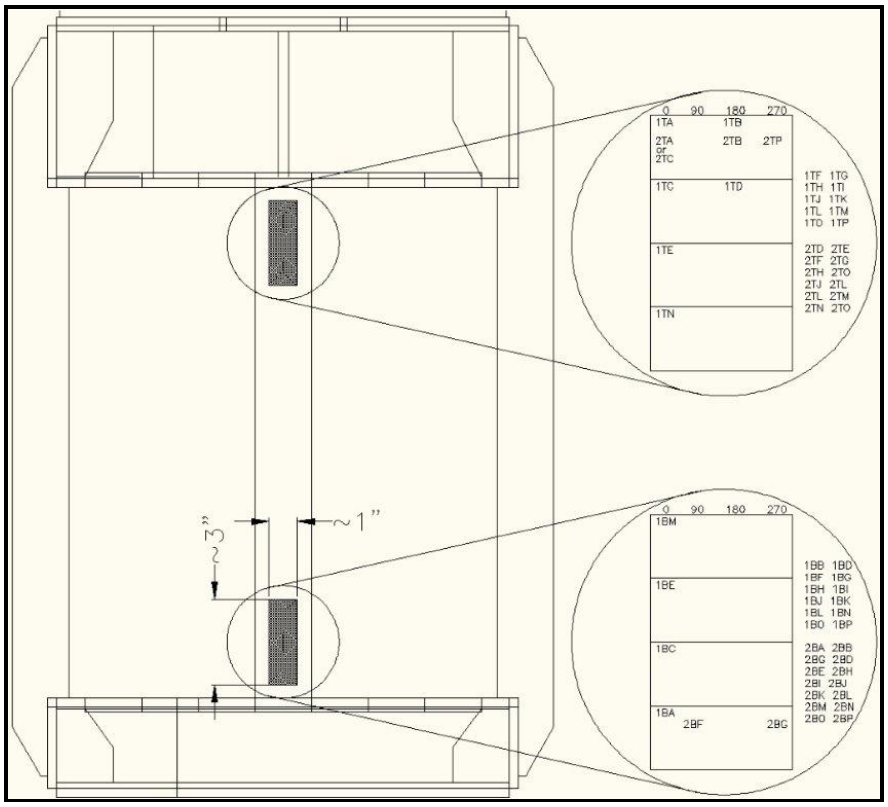

Figure 2-3 Mapping of Coupon Location Elevations and Quadrants

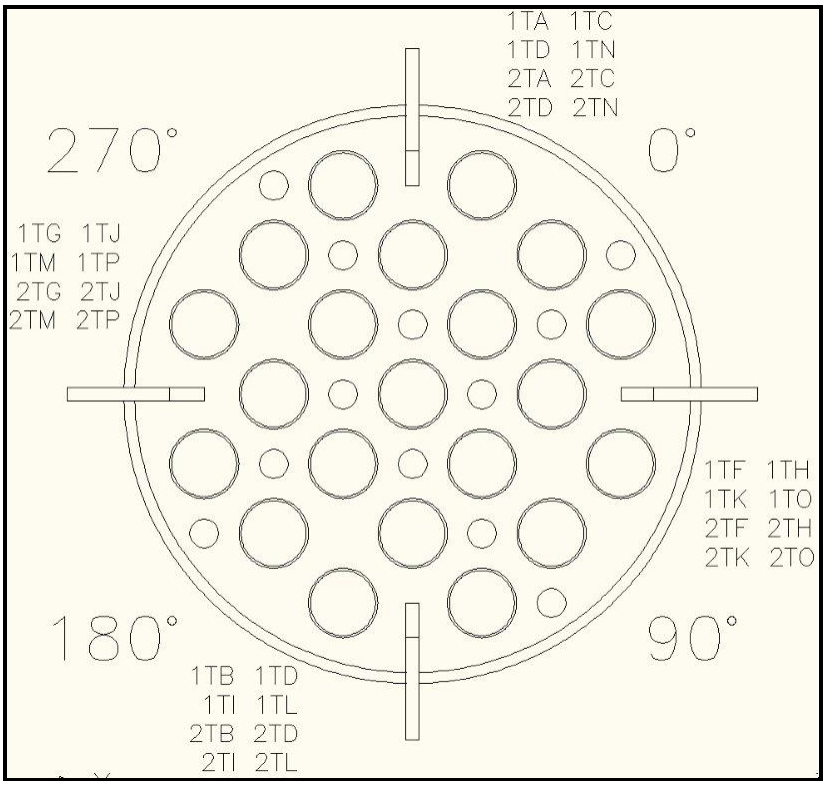

Figure 2-4 Mapping of Coupon Location Quadrants

2.3 Filter Coupon Leaching and Analysis: ICP-AES, IC, TIC, Radchem

A series of coupons were individually leached in approximately 100 mL of 3M HNO_3 for 72 hours. The acid leachates were then subsampled and submitted to Analytical Development (AD) for analysis by inductively coupled plasma – atomic emission spectroscopy (ICP-AES), Pu-238 and Pu-239/240, and for Sr-90 measurements. A separate series of coupons were individually leached in approximately 100 mL of deionized water for 72 hours. The water leachates were then subsampled and submitted to AD for analysis by ion chromatography (IC), total inorganic carbon – total organic carbon (TICTOC), and ICP-AES. The results [6] for both sets of leachate analyses were then normalized to one square inch of filter material (considering only one surface of the filter coupon, that corresponding to the inside surface of the filter tube) and expressed as either mg/sq. in. or dpm/sq. in. In the case of inorganic carbon, the result was also converted to a carbonate (CO_3^{2-}) basis.

2.4 Filter Coupon Non-Destructive Examination: XRD, XRF, SEM-EDS, FTIR

Separate filter coupons from those used in the leaching tests, were submitted for x-ray diffraction (XRD) spectroscopy, x-ray fluorescence (XRF) spectroscopy, scanning electron microscopy – energy dispersive spectroscopy (SEM-EDS), and Fourier transform infrared (FTIR) spectroscopy.

Four coupons from each filter were submitted for both XRD and XRF measurements: 1TC, 1TD, 1BC, 1BD, 2TC, 2TD, 2BC, and 2BD. The inside and outside surfaces of these Filter 1 and 2 coupons were examined. The XRF spectra were not collected under vacuum, so Ar is present in the spectra since it is present in the atmosphere.

In the case of SEM-EDS, the inside surface and the "snapped" edge of the following filter coupons were examined: 1BA, 1TA, 1BB, 1TB, 2BA, 2TA, 2BB, and 2TB. Additionally, the outside surface of coupon 2TB was examined.

FTIR measurements were made initially by looking at the surface solids, then removing the top layer of salt deposits to examine the layer beneath. Raman spectra could not be obtained on the coupons due to fluorescence from the coupons when placed in the instrument.

2.5 Quality Assurance

Requirements for performing reviews of technical reports and the extent of review are established in manual E7 2.60. SRNL documents the extent and type of review using the SRNL Technical Report Design Checklist contained in WSRC-IM-2002-00011, Rev. 2.

3.0 Results and Discussion

3.1 Visual Filter Inspection

On the left of Figure 3-1 is the filter bundle top as viewed from the four inch input line, and on the right is the interior view of an individual two inch filter tube.. As can be observed in this figure, there is no heavy scale build up on the filter walls when viewed from the top at the interior bundle assembly (left image in figure) or further down an individual filter tube (right image in figure). A scattering of white solids is visible, but they are reasonably evenly distributed, and appear to be salt deposits from evaporated feed solution that dried on the walls, likely after the removal of the filter from service. The heavy scale

coating noted previously[7] during an examination of an earlier secondary filter (guard filter) was not observed in either Filter 1 or Filter 2.

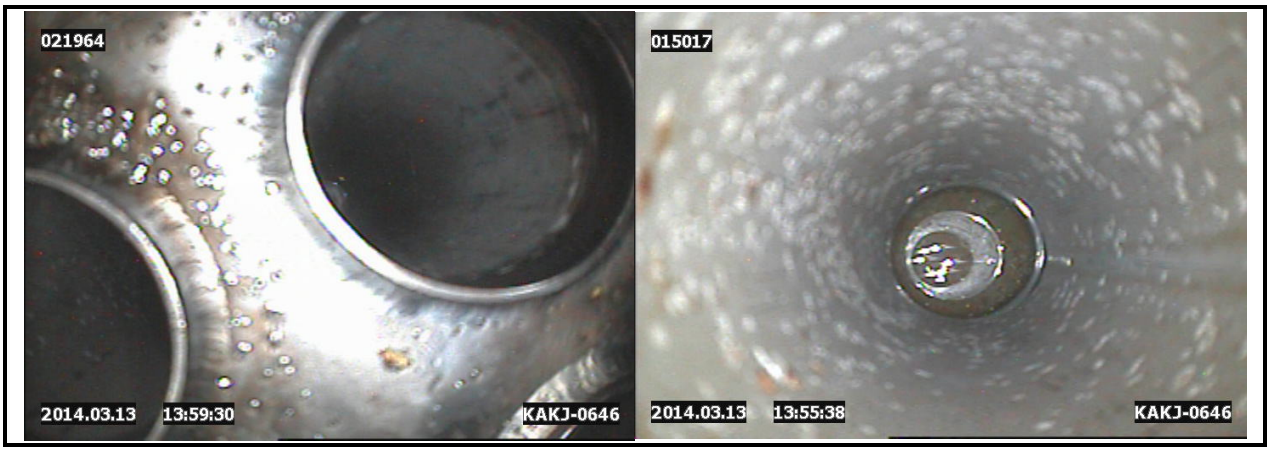

Figure 3-1 Interior View of Filter 1. Left image is taken from the top of the filter bundle. Right image is taken within one filter tube.

3.2 Filter Sampling

The filter cutting operation did result in the portion of the filter adjacent to the oscillating tool becoming red hot. This extreme heating would be expected to have some impact on the chemical constituents on the filter surface and interior void spaces, but it is difficult to quantify the impact in the absence of a control coupon that was exposed to the same processing conditions, but not the temperature excursion.

Since the focus was to identify significant changes in chemistry, no special precautions were taken to avoid cross-contamination from either the Shielded Cells manipulator fingers, beyond wiping the fingers clean prior to handling and subsample the initial filter, or from the in-cell vice used to break the coupon strips into individual coupons. Hence it is important to not over interpret any trace constituents found on coupons produced from either filter.

Since uncertainties developed in the exact positions within the subsectioned top or bottom coupons, the stratification determination or interpretation is more difficult. Generally, comparisons will be limited to top vs. bottom and Filter 1 vs. Filter 2.

3.3 Leached Filter Coupon Analyses: ICP-AES, IC, TIC, and Radchem

Table 3-1 contains the Pu-238, Pu-239/240, Sr-90, and ICP-AES elemental composition determined for each coupon that was leached in acid. Only elements with measurements above the instrument detection limit were included in the table, though there may be some individual coupons where a particular metal ion concentration was below the detection limit of the instrument. The elemental and radiochemical data generally showed a great deal of spread in the measurements, which is apparent if one reviews the high %RSD determined across coupons taken in the same region (top vs. bottom) of the either filter. Data are reported on the basis of the surface area of one side of the filter coupon (i.e., relating to the area on the inner surface of the filer tube). Small measurement errors in the coupon dimensions, that were measured to the nearest 1/8th inch, would contribute to the high %RSD values.

Some general observations can be made. Filter 1 had more metal ion deposits than did Filter 2, even though Filter 1 proceesed a smaller number of salt batches, hence this may reflect the impact of having rinsed Filter 2 prior to sending it to SRNL for analysis. The relative abundance of elements in the acid leachates is as follows for each filter:

Na > Fe > Ti > Al > Ni *Filter 1*

Na > Fe > Ti > Ni > Al *Filter 2*

The Fe and Ni are likely leached from the stainless steel sintered metal filter, but Na, Ti, and Al are likely from the salt batch being processed. The amount of iron found between the two filters is nearly identical, while the amount of Ni found was slightly higher for Filter 2. Interestingly, the ratio of Ti:Al was 1.1 for Filter 1, but the Ti:Al ratio for Filter 2 was 4.1. Filter 1 had more Al and Na compared to Filter 2, while Filter 2 had more Ba, Ca, P, Th, and Ti compared to Filter 1. Generally, the bottom coupons from a filter tube had higher elemental composition than did the coupons originating from the top, though there is a notable exception with Al, especially in Filter 1, where the top coupons had roughly 2x the bottom coupon deposition of Al.

The coupons of Filter 2 had more Pu activity than those of Filter 1 by a factor of roughly two. This observation did not hold for Sr-90 activity between the two filters, where activity levels were approximately equivalent. See comparison in Table 3-2. When the measured activity of Pu-238 is converted to mass using the specific activity of 17.12 Ci/g,[8] the ratio of Ti:Pu-238 is reasonably consistent between the tops of each filter and the bottoms of each filter. See comparison in Table 3-3. This comparison cannot be made for the Pu-239 or Pu-240 isotopes since the activities were not resolved and hence cannot be converted to mass equivalents.

Table 3-1 Elemental and Radiochemical Composition of Acid Leached Coupons for Filter 1 (F1) and Filter 2 (F2)

Coupon ID	Pu-238	Pu-239/240	Sr-90	Al	Ba	Ca	Cd	Co	Cr	Fe	Mn	Na	Ni	P	Si	Th	Ti	Zn
	dpm/sq in	dpm/sq in	dpm/sq in	mg/sq in	mg/sq in	mg/sq in	mg/sq in	mg/sq in	mg/sq in	mg/sq in	mg/sq in	mg/sq in	mg/sq in	mg/sq in	mg/sq in	mg/sq in	mg/sq in	mg/sq in
1TH	1.05E+06	1.55E+05	1.04E+07	2.46	<0.00712	0.0262	0.0198	<0.0125	0.210	1.72	0.0472	15.8	0.545	<0.255	0.169	<0.0591	1.87	0.00931
1TI	1.33E+06	1.38E+05	1.45E+07	2.15	<0.0107	0.0163	0.0212	<0.0187	0.172	1.44	0.0304	14.2	0.505	<0.382	<0.181	<0.0886	1.84	0.0143
1TJ	1.93E+06	2.04E+05	1.66E+07	2.89	<0.0107	0.0321	0.0310	0.0235	0.591	5.88	0.216	23.5	1.40	<0.382	0.310	<0.0887	2.75	0.0186
F1 Top Ave [%RSD]	**1.44E+06 [31]**	**1.66E+05 [21]**	**1.38E+07 [23]**	**2.50 [15]**	**<0.00712**	**0.0248 [32]**	**0.0240 [26]**	**0.0235 [NA]**	**0.324 [71]**	**3.02 [82]**	**0.0978 [105]**	**17.8 [28]**	**0.817 [62]**	**<0.255**	**0.239 [42]**	**<0.0591**	**2.15 [24]**	**0.0141 [33]**
1BH	1.89E+06	1.91E+05	1.64E+07	1.38	<0.00641	0.0216	0.0213	0.0128	0.394	2.44	0.135	26.5	0.872	<0.229	0.176	<0.0532	1.97	0.0115
1BI	2.05E+06	2.17E+05	2.04E+07	0.928	<0.00908	0.0363	0.0241	0.0148	0.506	3.65	0.204	20.3	1.11	<0.325	0.434	<0.0754	2.24	0.0144
1BJ	1.74E+06	1.75E+05	1.20E+07	1.53	<0.00797	0.0484	0.0233	0.0281	0.687	7.09	0.176	23.5	2.03	<0.285	0.593	<0.0661	2.23	0.0178
F1 Bottom Ave [%RSD]	**1.89E+06 [8.2]**	**1.94E+05 [11]**	**1.62E+07 [26]**	**1.28 [25]**	**<0.00641**	**0.0355 [38]**	**0.0229 [6.2]**	**0.0185 [45]**	**0.529 [28]**	**4.39 [55]**	**0.172 [20]**	**23.4 [13]**	**1.34 [46]**	**<0.229**	**0.401 [52]**	**<0.0532**	**2.15 [7.0]**	**0.0146 [22]**
2TH	2.58E+06	2.99E+05	1.39E+07	1.21	0.0610	0.0433	0.0222	<0.0188	0.489	2.96	0.0371	16.9	1.01	<0.385	0.406	0.109	3.58	0.0151
2TI	1.24E+06	1.32E+05	4.04E+06	0.839	0.0609	0.0340	0.0175	<0.0214	0.355	2.82	0.0277	14.5	0.962	<0.438	<0.208	<0.102	1.79	0.0135
2TJ	2.03E+06	2.34E+05	1.48E+07	0.809	0.0590	0.0484	0.0242	0.0167	0.637	3.61	0.119	11.3	1.18	0.171	0.271	0.0892	3.56	0.0158
F2 Top Ave [%RSD]	**1.95E+06 [34]**	**2.21E+05[38]**	**1.09E+07 [55]**	**0.954 [24]**	**0.0603 [1.9]**	**0.0419 [17]**	**0.0213 [16]**	**0.0167 [NA]**	**0.494 [29]**	**3.13 [13]**	**0.0613 [82]**	**14.2 [20]**	**1.05 [11]**	**0.171 [NA]**	**0.338 [28]**	**0.0989 [14]**	**2.98 [35]**	**0.0148 [8.1]**
2BH	4.49E+06	5.14E+05	2.45E+07	0.745	0.0516	0.0447	0.0330	0.0202	0.825	4.24	0.155	16.6	1.63	0.339	<0.155	0.0830	3.60	0.0180
2BI	4.81E+06	5.33E+05	1.39E+07	0.868	0.0852	0.0731	0.0446	0.0193	0.683	4.82	0.0638	17.7	2.02	0.246	<0.0890	0.130	5.08	0.0231
2BJ	4.30E+06	4.42E+05	1.57E+07	0.670	0.0515	0.0648	0.0345	0.0152	0.843	4.33	0.107	15.1	1.65	0.123	0.169	0.0945	3.67	0.0201
F2 Bottom Ave [%RSD]	**4.53E+06 [5.6]**	**4.96E+05 [10]**	**1.80E+07 [31]**	**0.761 [13]**	**0.0628 [31]**	**0.0609 [24]**	**0.0374 [17]**	**0.0182 [15]**	**0.784 [11]**	**4.46 [7.0]**	**0.109 [42]**	**16.5 [8.0]**	**1.77 [13]**	**0.236 [46]**	**0.169 [NA]**	**0.103 [24]**	**4.12 [20]**	**0.0204 [13]**

Table 3-2 Comparison of Filter 1 and 2 Radionuclide Activities

Species	Filter 1 dpm/sq. in.	Filter 2 dpm/sq. in.
Pu-238	1.67E+06	3.24E+06
Pu-239/240	1.80E+05	3.59E+05
Sr-90	1.50E+07	1.45E+07

Table 3-3 Comparison of Ti:Pu-238 Ratios for Filter 1 and 2

	Top	Bottom
Filter 1	5.7E+04	4.3E+04
Filter 2	5.8E+04	3.5E+04

Table 3-4 contains the measured elemental and anion distribution for the water leached coupons. Only elements and anions measured in either Filter 1 or Filter 2 leachates at values above the instrument detection limit have been included in the table. As can be seen from surveying the %RSD values in the table (range 3 to 64), there is a large degree of variability in the measured values obtained from the individual coupons.

Filter 1 had roughly twice the distribution of anion salts when compared with Filter 2 (see last two rows of Table 3-4). Also, there was no oxalate ion value above the detection limit measured for Filter 1. The data in the table assumes that any inorganic carbon measured could be attributed solely to carbonate. It should be noted that the carbonate distribution measured may actually be produced **after** the filter is removed from service. Any residual high caustic solution on the filter would adsorb atmospheric carbon dioxide and produce bicarbonate and carbonate salt deposits on the filter upon drying.

$$Na^{+}_{(aq)} + OH^{-}_{(aq)} + CO_{2(g)} \rightleftharpoons Na^{+}_{(aq)} + HCO_3^{-}{}_{(aq)} \qquad \textbf{Equation 1}$$

Based on the water leachate results, there is twice the Al and Na distribution on Filter 1 relative to Filter 2, and this difference is likely significant even in light of the high variability between individual coupons. Prior to receipt by SRNL, Filter 2 was rinsed with water, while Filter 1 was not rinsed.

Table 3-4 Elemental and Anion Composition of Water Leached Coupons for Filter 1 and 2

Coupon ID	CO_3^{2-} mg/sq in	NO_2^- mg/sq in	NO_3^- mg/sq in	SO_4^{2-} mg/sq in	$C_2O_4^{2-}$ mg/sq in	Al mg/sq in	Cr mg/sq in	Fe mg/sq in	Na mg/sq in
1TK	40	6.3	38	1.8	<0.39	0.715	<0.0244	<0.00723	35.9
1TL	15	2.4	15	0.67	<0.10	0.198	<0.00650	<0.00193	14.3
1TM	30	4.5	28	1.4	<0.41	0.998	0.0524	<0.00753	26.8
Filter 1 Top Average [%RSD]	**29 [45]**	**4.4 [44]**	**27 [44]**	**1.3 [44]**	**<0.10**	**0.637 [64]**	**0.0524 [NA]**	**<0.00193**	**25.7 [42]**
1BK	21	3.7	24	1.1	<0.27	0.438	0.0470	<0.00492	20.6
1BL	21	4.0	21	1.2	<0.20	0.431	0.0986	0.00443	21.3
1BM	25	4.9	30	1.6	<0.20	0.651	0.0803	<0.00363	28.6
Filter 1 Bottom Average [%RSD]	**22 [11]**	**4.2 [15]**	**25 [18]**	**1.3 [19]**	**<0.20**	**0.507 [25]**	**0.0753 [35]**	**0.00443 [NA]**	**23.5 [19]**
2TK	15	1.7	10	0.54	0.26	0.290	0.169	0.00313	12.3
2TL	18	2.6	15	0.71	0.090	0.288	0.0657	<0.00166	16.8
2TM	21	2.6	15	0.73	0.39	0.304	0.281	0.00600	17.8
Filter 2 Top Average [%RSD]	**18 [18]**	**2.3 [23]**	**13 [24]**	**0.66 [15]**	**0.25 [61]**	**0.294 [3.1]**	**0.172 [63]**	**0.00457 [45]**	**15.6 [19]**
2BK	14	2.5	15	0.71	0.26	0.281	0.203	<0.00243	16.3
2BL	11	1.4	7.8	0.39	<0.10	0.195	0.0555	<0.00181	9.82
2BM	18	1.8	11	0.53	0.39	0.201	0.219	<0.00363	12.9
Filter 2 Bottom Average [%RSD]	**14 [23]**	**1.9 [30]**	**11 [31]**	**0.55 [29]**	**0.33 [28]**	**0.226 [21]**	**0.159 [57]**	**<0.00181**	**13.0 [25]**
Filter 1 Average [%RSD]	**26 [35]**	**4.3 [30]**	**26 [31]**	**1.3 [30]**	**<0.10**	**0.572 [49]**	**0.0696 [35]**	**0.00443 [NA]**	**24.6 [31]**
Filter 2 Average [%RSD]	**16 [22]**	**2.1 [26]**	**12 [26]**	**0.60 [22]**	**0.28 [45]**	**0.260 [19]**	**0.166 [54]**	**0.00457 [45]**	**14.3 [22]**

3.4 Un-Leached Filter Coupon Analyses: XRD, XRF, SEM-EDS, FTIR

3.4.1 XRD

Both Filter 1 and 2 coupons were examined by XRD. Figure 3-2 shows the XRD spectra collected for the inside surface of Coupons 1TC and 1TD, and Figure 3-3 show the spectra collected for the inside surface of Coupons 1BC, and 1BD. The only species measured by XRD on the inside surface of both top coupons (Figure 3-2) is a combination of sodium carbonate and sodium nitrate, specifically, $Na_2CO_3 \bullet H_2O$ (Thermonatrite) and $NaNO_3$ (Nitratine). The species labeled Taenite (Fe, Ni) is a result of the 316L sintered stainless steel filter media. The most likely source of the two deposited materials is crystallization of Na salts of carbonate and nitrate, the former formed post processing and the latter from the process salt batch. Any other materials present on the coupons were likely at too low a concentration for XRD to detect or were non-crystalline species.

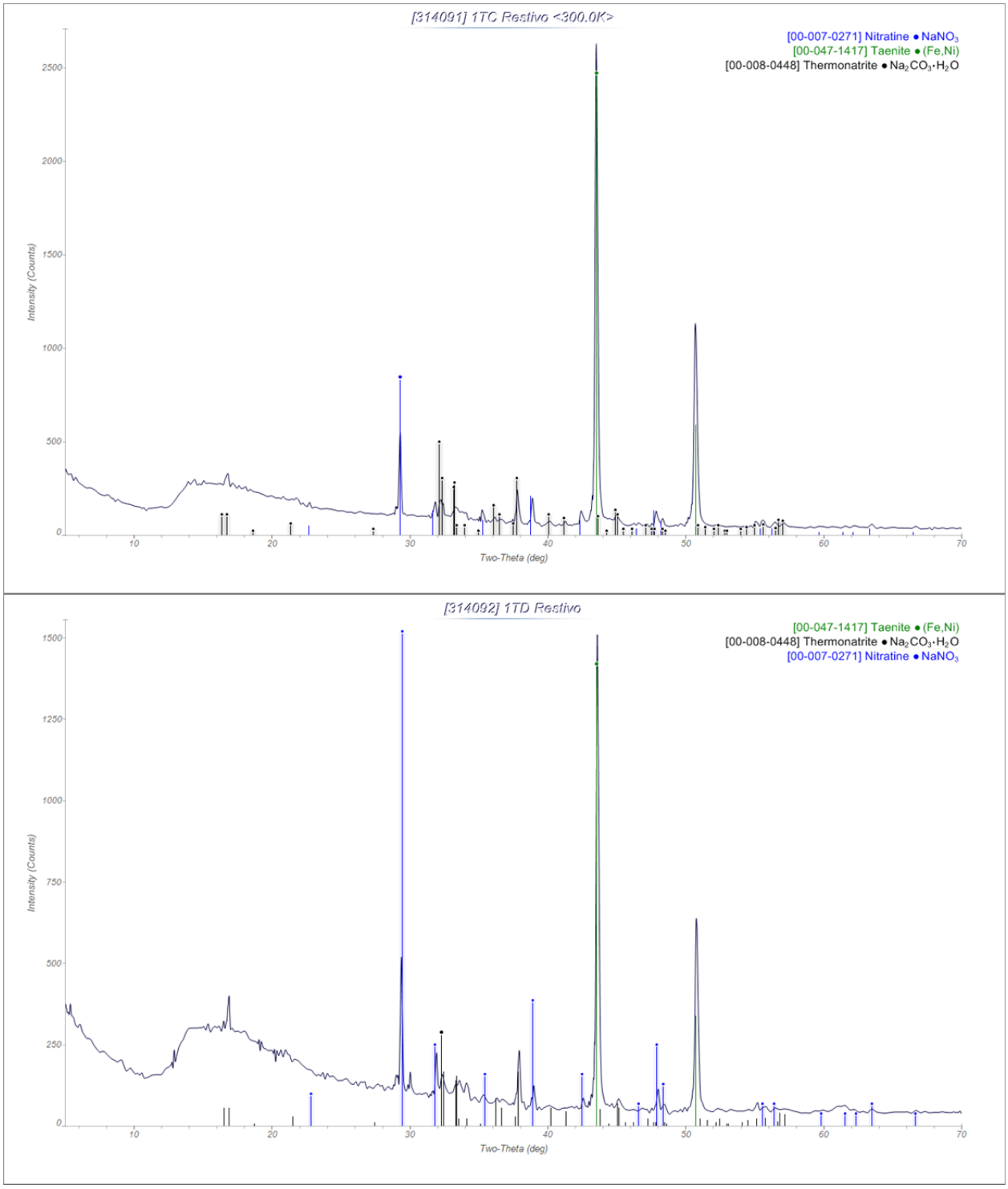

Figure 3-2 XRD Spectra for Filter 1, Coupons 1TC and 1TD

For the two bottom coupons the inside surface revealed salts of bicarbonate and nitrite, specifically, $Na_3H(CO_3)_2 \bullet 2H_2O$ (Trona) and $NaNO_2$ (sodium nitrite), in addition to those of carbonate and nitrate observed on the top coupons.

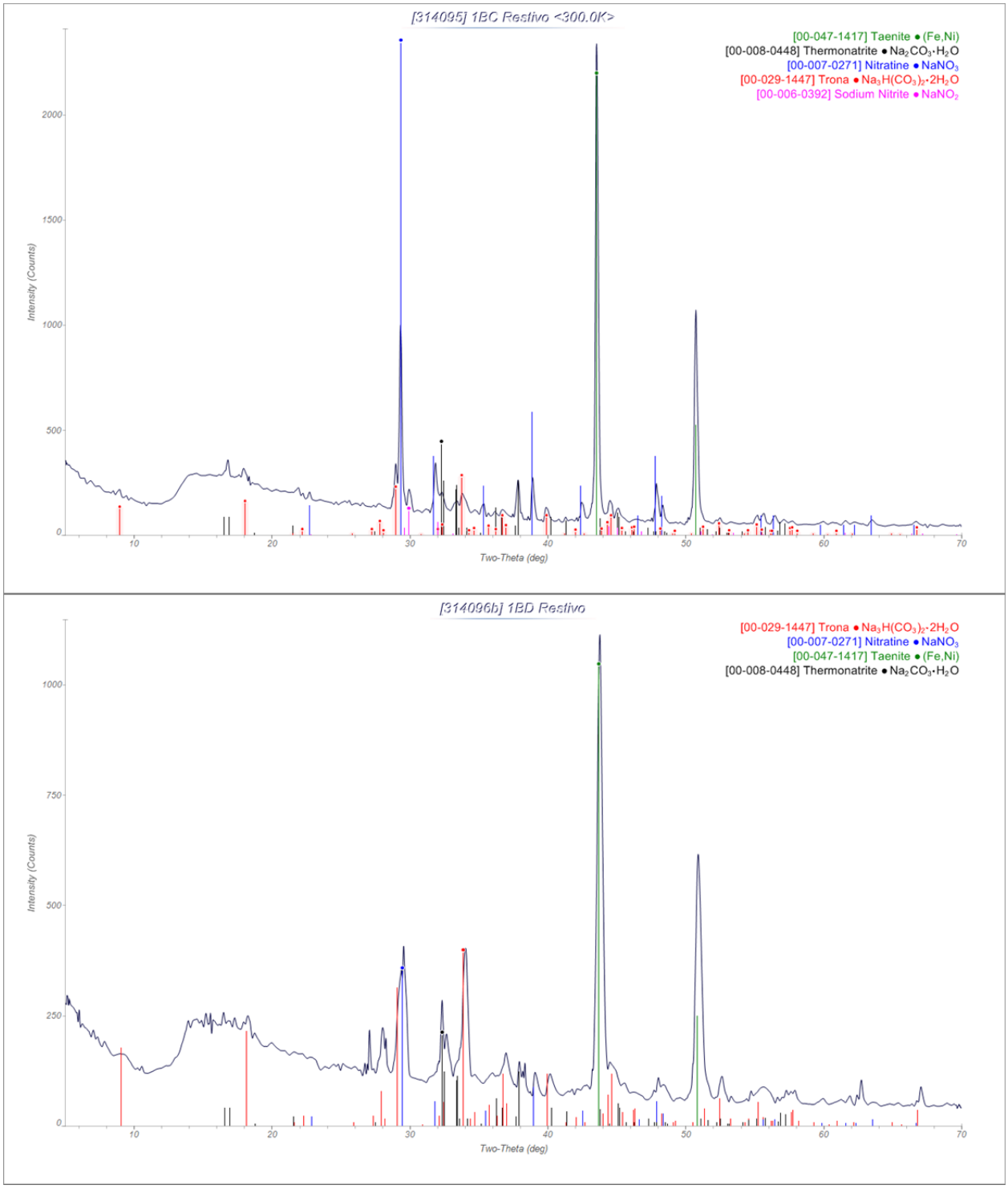

Figure 3-3 XRD Spectra for Filter 1, Coupons 1BC and 1BD

The XRD spectra collected for the inside surface of the Filter 2 coupons are given in Figure 3-4 and Figure 3-5. For the two top coupons the inside surface revealed only sodium nitrate (Natratine) in addition to the stainless steel (Taenite).

.

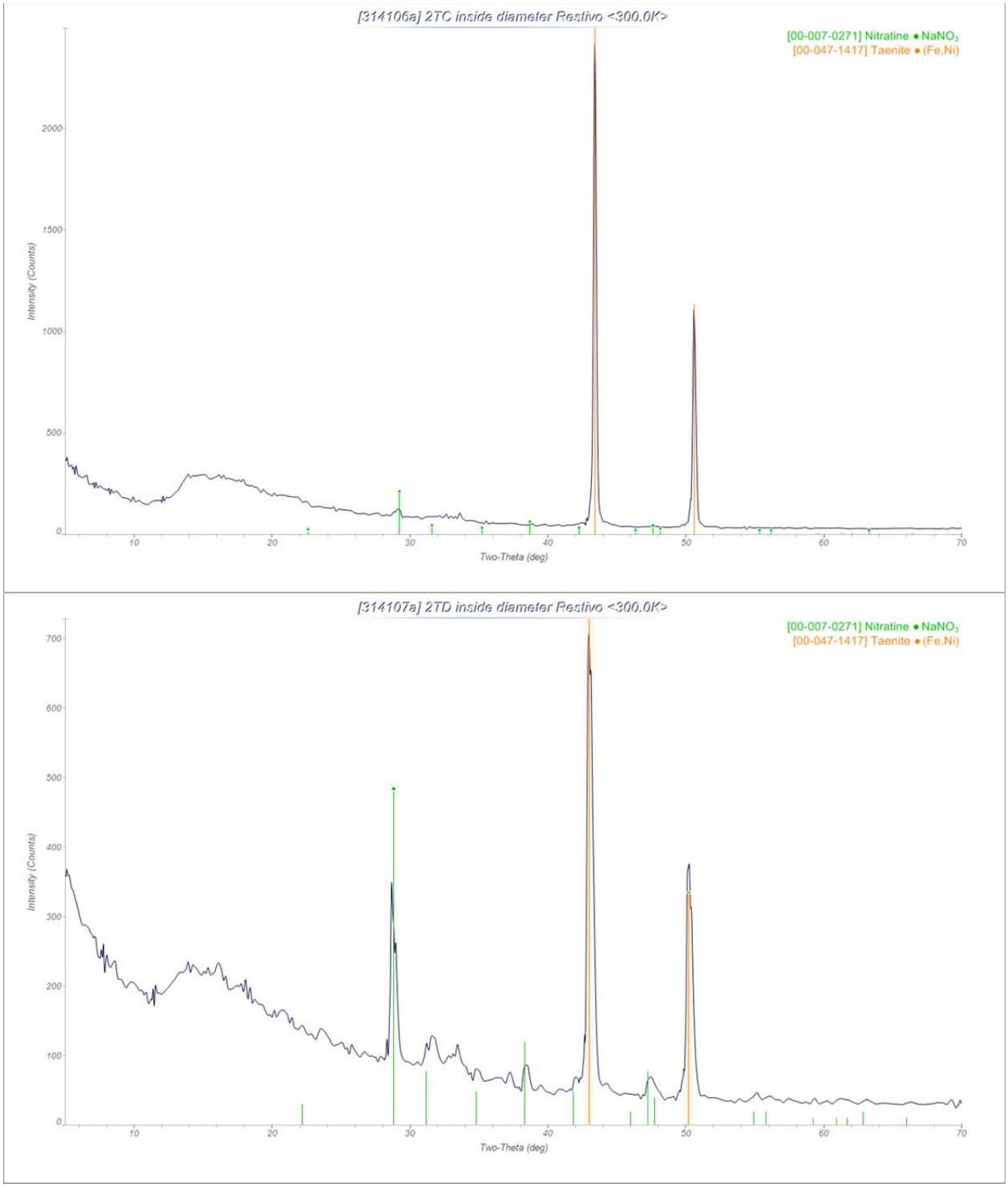

Figure 3-4 XRD Spectra for Filter 2, Coupons 2TC and 2TD

For the two bottom coupon inside surfaces from Filter 2 sodium bicarbonate, specifically $Na_3H(CO_3)_2 \bullet 2H_2O$ (Trona), was also detected in addition to the sodium nitrate and stainless steel. Again,

any other materials present on the coupons were likely at too low a concentration for XRD to detect or were non-crystalline species. The spectra obtained for Coupons 2BC and 2BD are given in Figure 3-5

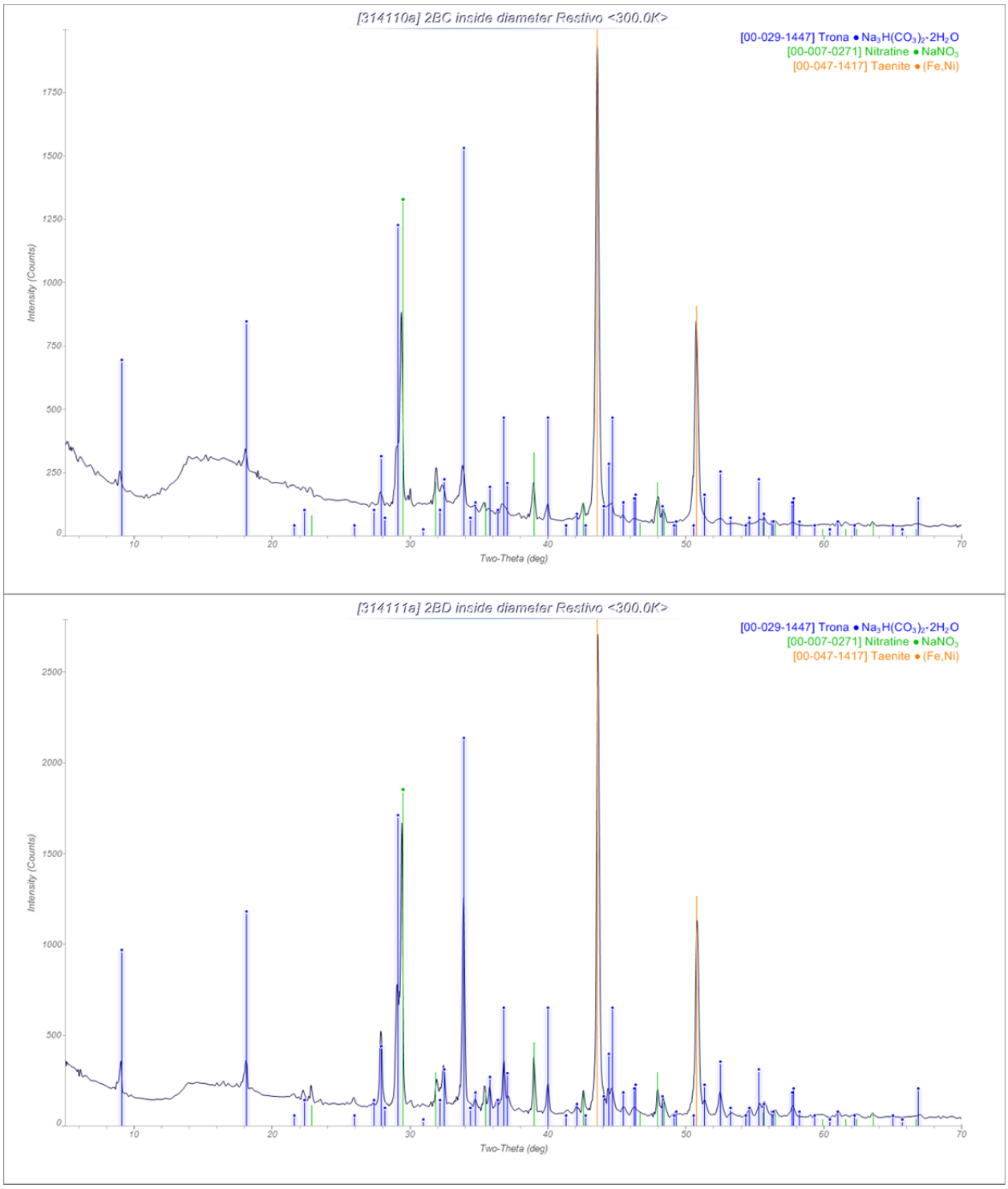

Figure 3-5 XRD Spectra for Filter 2, Coupons 2BC and 2BD

An examination by XRD of the outer surfaces of both top and bottom derived coupons revealed combinations of the same bicarbonate, carbonate, nitrate, and nitrite salts observed on the inside surfaces. One coupon gave a weak signal for sodium aluminum silicate (NAS), $Na_8(AlSiO_4)_6(NO_3)_2$. The spectra for this coupon, 2TC, is shown in Figure 3-6.

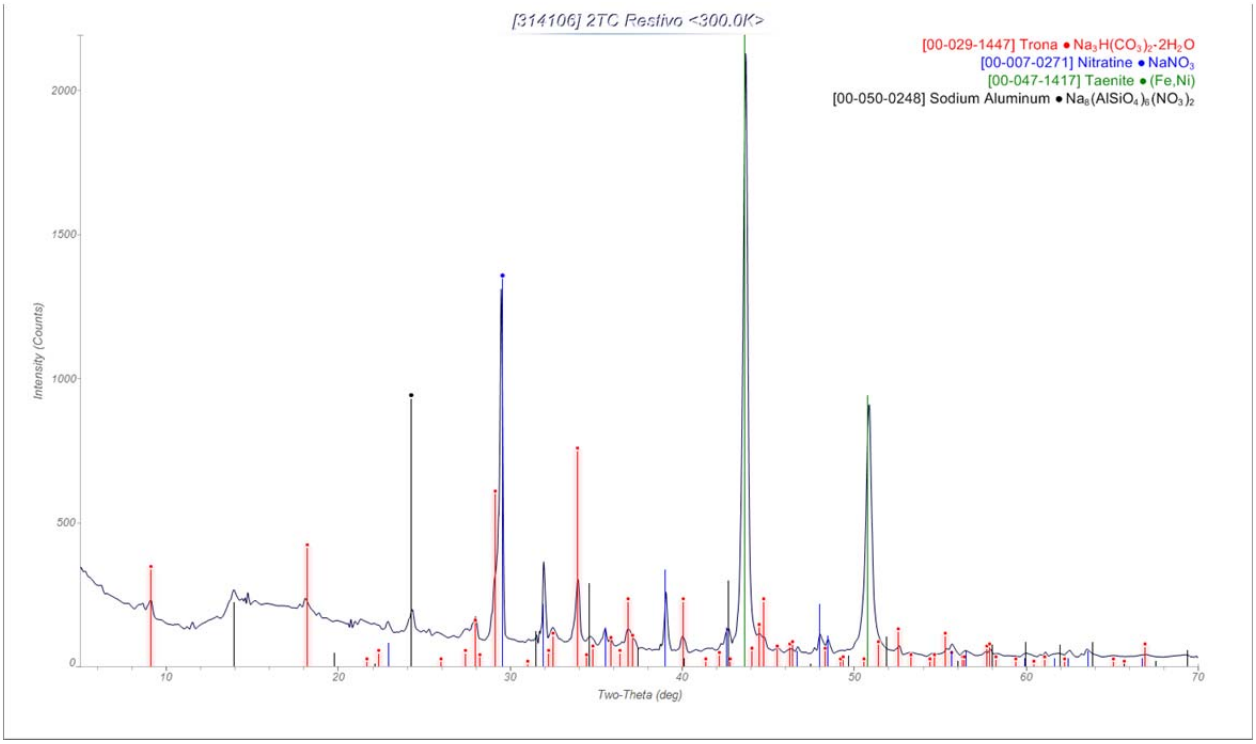

Figure 3-6 XRD Spectra for Filter 2, Coupon 2TC, Outside Surface

3.4.2 XRF

X-ray fluorescence spectra were collected on the same eight coupons for Filter 1 and 2 examined by XRD in the previous section. XRF was only a bit more successful at identifying materials on the interior surface of the coupons. A typical spectra is shown in Figure 3-7. It indicates that the major species present are due to the sintered, stainless steel filter material: Fe, Cr, Ni, and Mo.

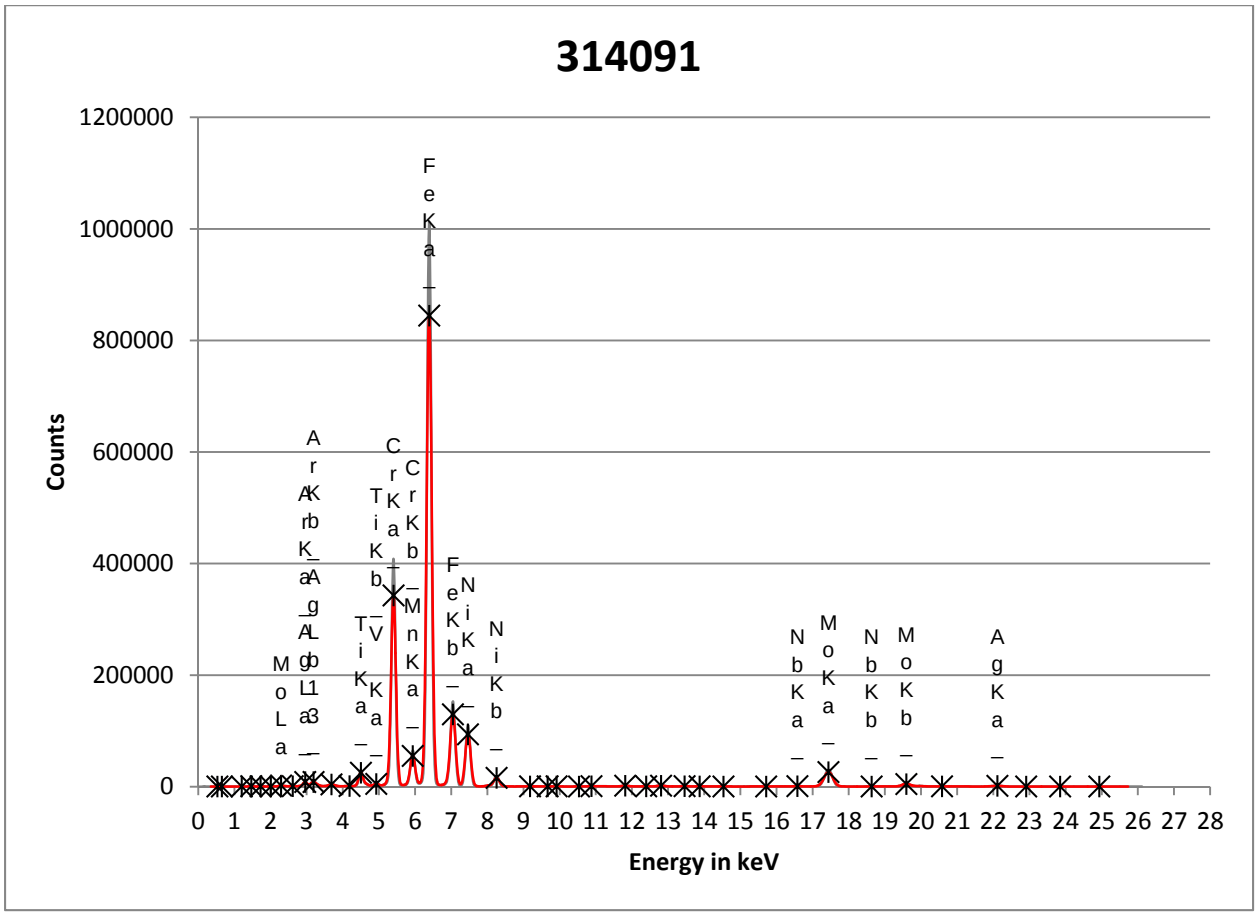

Figure 3-7 XRF Spectra for Filter 1, Coupon 1TC, Inside Surface

In an effort to identify minor species, we examined the close-up spectra for each of the coupons. These spectra for Filter 1 are shown in Figure 3-8 and Figure 3-9. The weak Ti signal seen in Figure 3-7 is now more clearly visible and comprised of two peaks. Weak signals for sludge components including As and/or Pb (cannot be differentiated) as well as S, Ag, Zr, and Nb are also present.

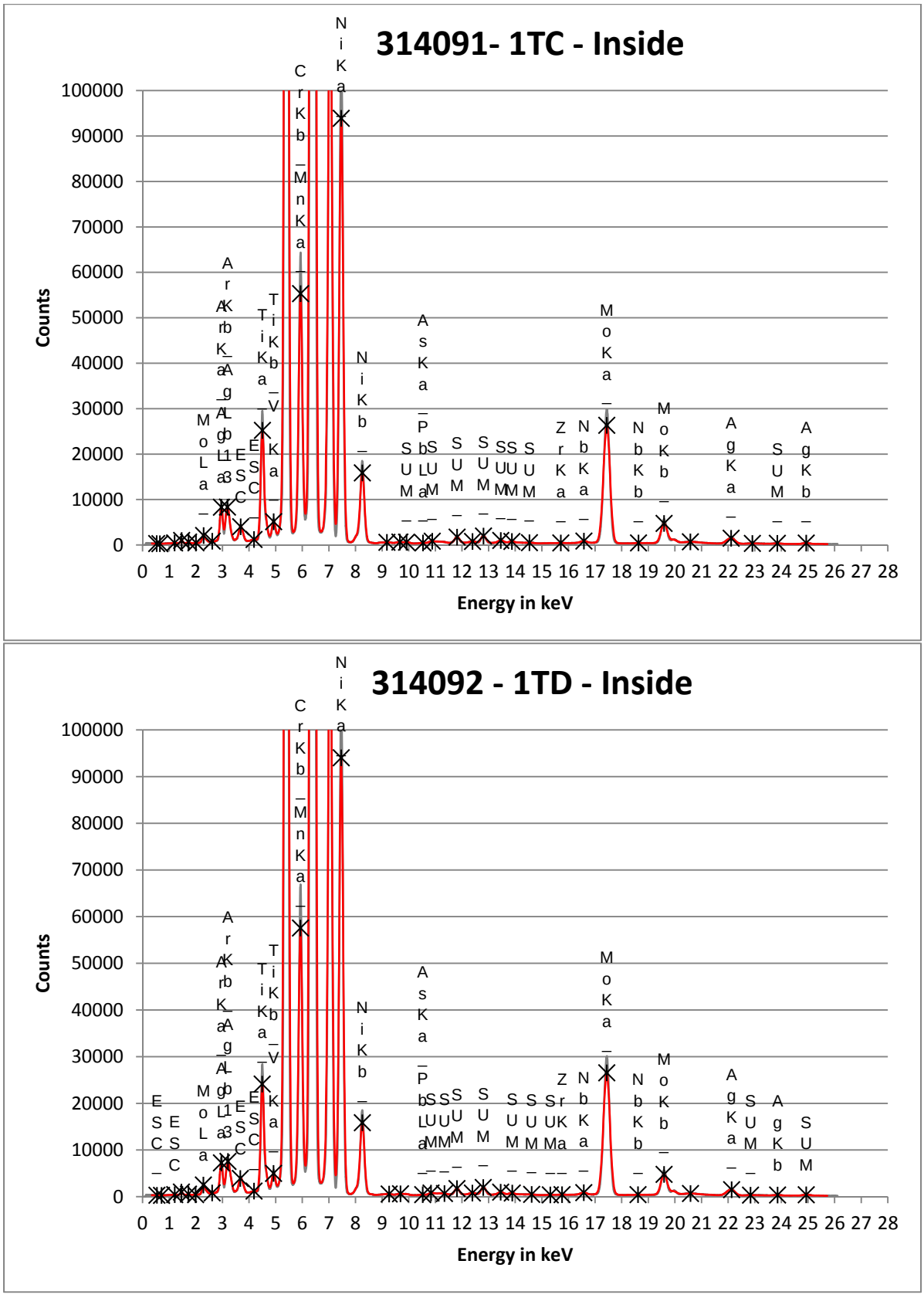

Figure 3-8 XRF Spectra for Filter 1, Coupons 1TC and 1TC, Inside Surface

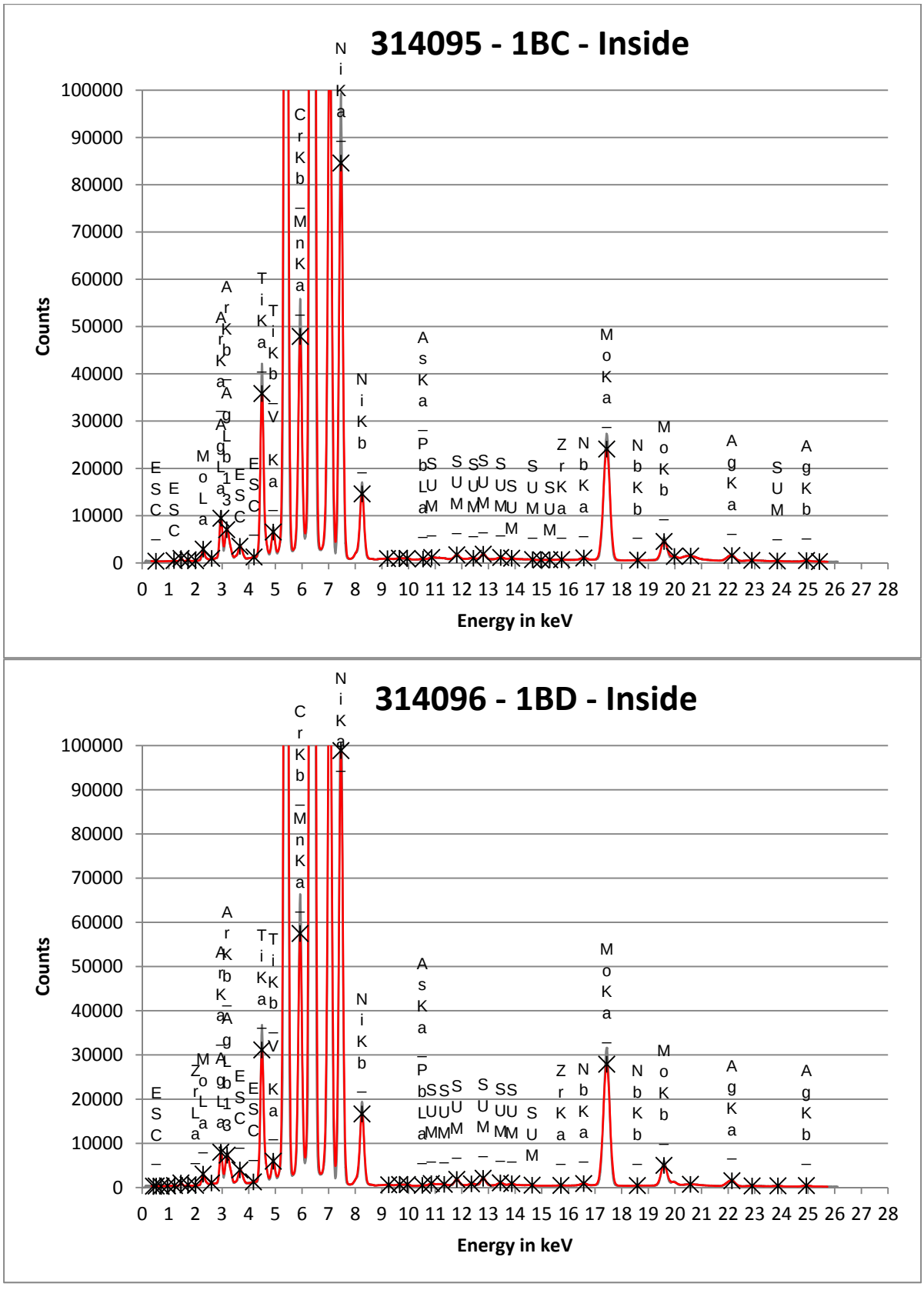

Figure 3-9 XRF Spectra for Filter 1, Coupons 1BC and 1BC, Inside Surface

The XRF spectra collected for Filter 2 are given in Figure 3-10 and Figure 3-11. In Figure 3-10 we have the spectra for the inside surface of the top two coupons, 2TC and 2TD. In addition to the Ti observed on the Filter 1 spectra, we also see Ca, S, and Hg, and traces of Ag, Al, Nb, and Zn in the top coupons. Al, Ca and Hg were not seen on Filter 1, and the signal here for S is stronger.

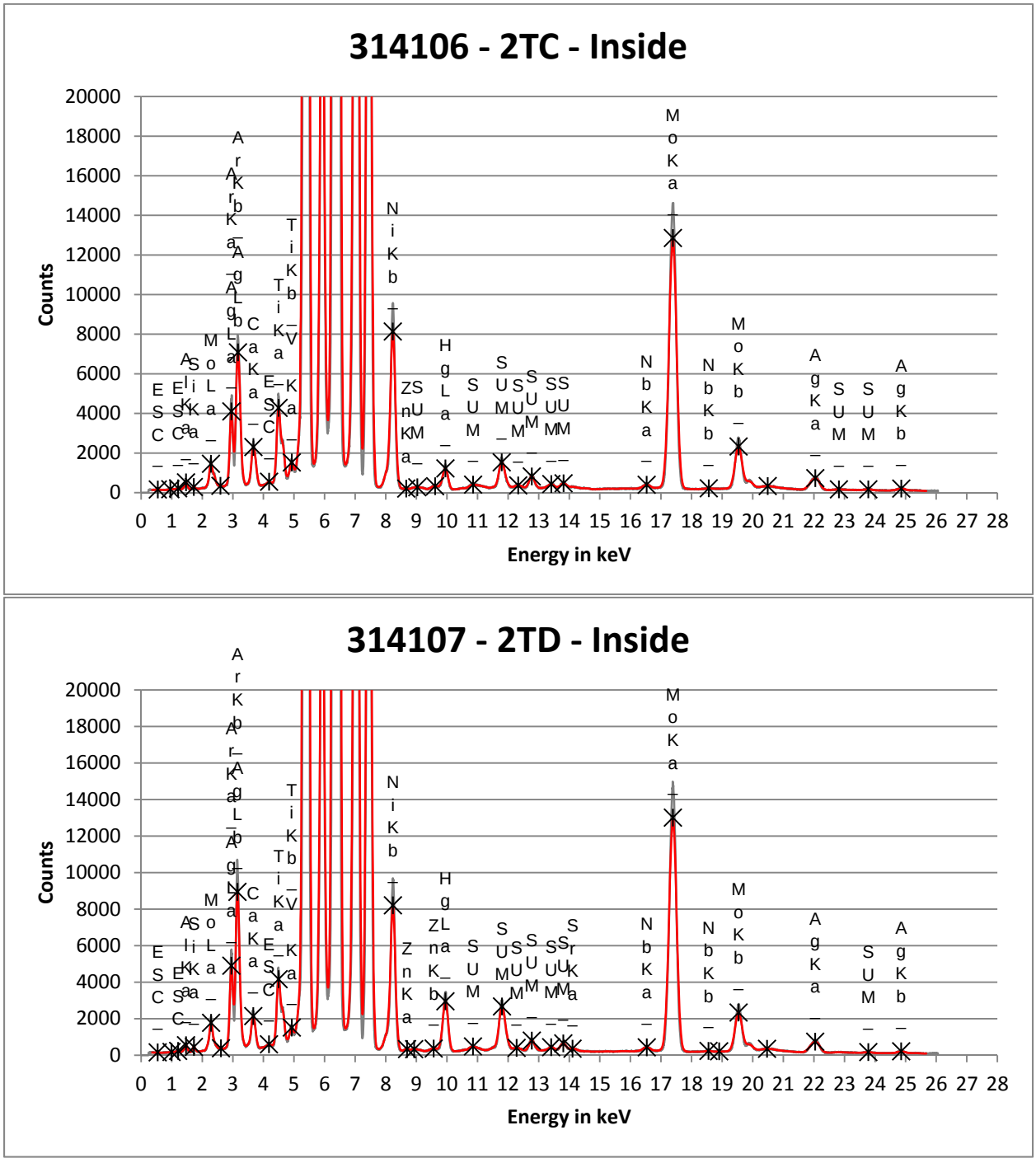

Figure 3-10 XRF Spectra for Filter 2, Coupons 2TC and 2TD, Inside Surfaces

In Figure 3-11. we have the spectra for the inside surface of the bottom two coupons, 2BC and 2BD. In addition to the Ti observed in the Filter 1 spectra and the top coupons for Filter 2, we also see sludge components including Ca, S, and Hg, and traces of Ag, Al, Ba, Ir, Nb, Rb, Si, Sr, and Zn in the top coupons. As was true for the bottom coupons for Filter 2, Al, Ca and Hg were not seen on Filter 1, and the signal for S was weaker. Neither Filter 1 coupons, nor the top Filter 2 coupons had a measurable signal from Ba, Ir, Rb, Si or Sr.

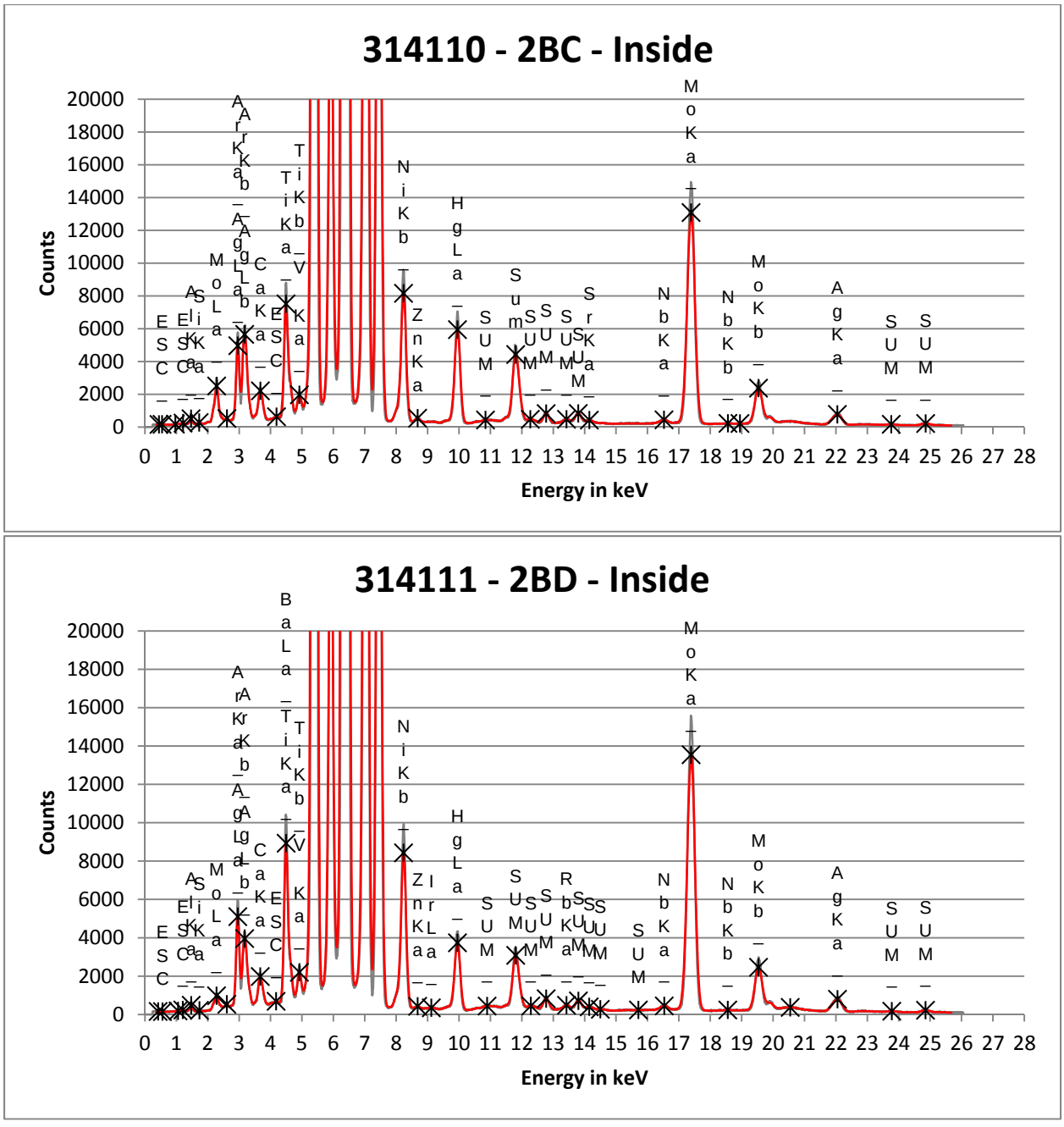

Figure 3-11 XRF Spectra for Filter 2, Coupons 2BC and 2BD, Inside Surfaces

A comparison coupon 2BC's inside and outside surfaces is made in Figure 3-12. Interestingly, while the sintered stainless steel elements are consistent between the two surfaces, as they should be, there is also a significant signal on the external surface for Al, Ca, Hg, and Ti amongst other trace elements. Either fine particles are working their way through the secondary filter and thus appearing on the external surface, and/or there was cross-contamination from the two surfaces during sample collection, handling, and analysis. It should be noted that these secondary filters hang in the LWHT and are therefore in constant contact with the tank solution. Either way, we see little difference in the XRF spectra between the inner and external surfaces of the coupons analyzed.

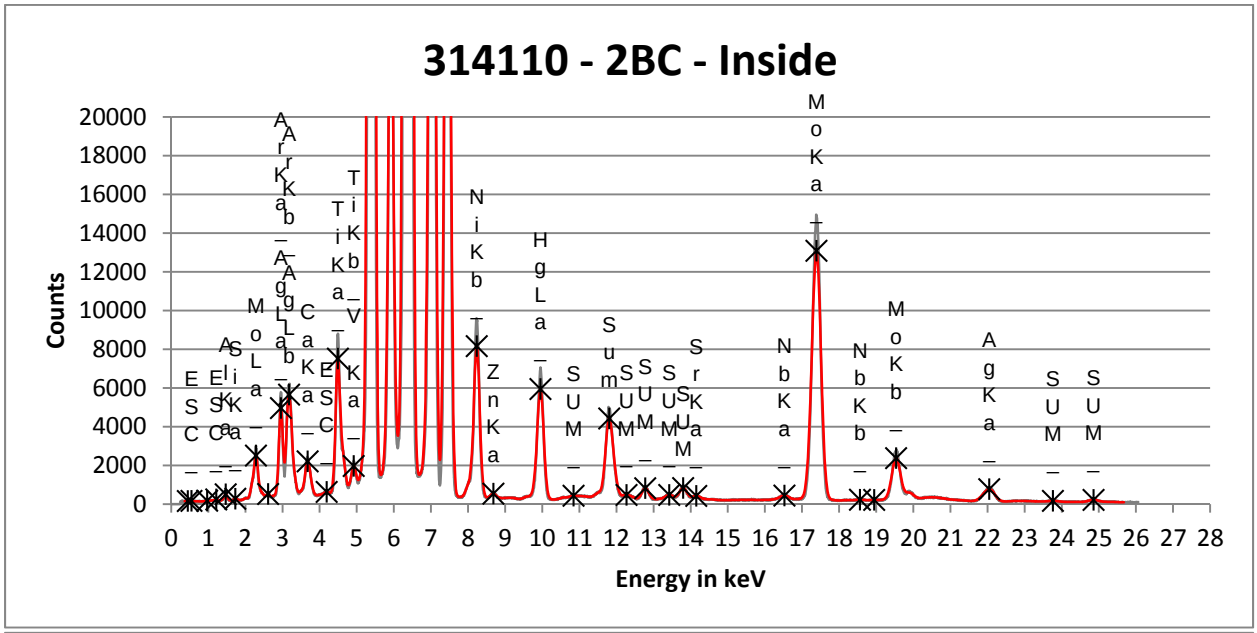

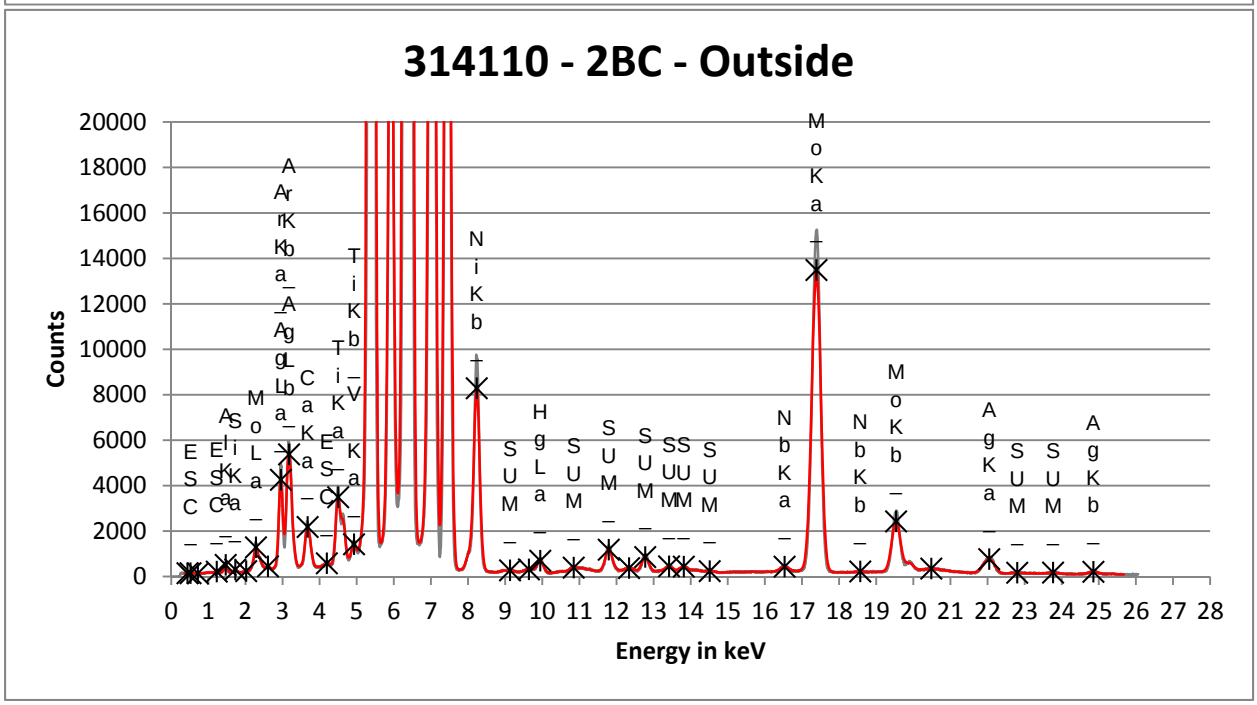

Figure 3-12 XRF Spectra for Filter 2, Coupon 2BC, Comparing Inside and Outside Surfaces

3.4.3 SEM-EDS

A vast array of photomicrographs and EDS spectra were collected on the eight coupons submitted for contained SEM analysis: (Filter 1) 1TA, 1TB, 1BA, 1BB; (Filter 2) 2TA, 2TB, 2BA, 2BB. Due to the large number of images and spectra, only a representative selection of the results will be recorded here. All data obtained for these samples are contained in the SRNL E-Notebook system.[4, 5, 6, 9, 10, 11, 12, 13, 14, 15,16] Some general observation:

- The SEM images did not indicate the presence of a scale coating on the inside surface of the filter for any of the coupons collected from either filter [Note, they were not examined visually to any great degree];
- The inside surface debris appears as a fine, powdery coating interspersed with crystalized salt deposits that is often penetrated by the electron beam during EDS data collection – hence the underlying stainless steel media is also analyzed in most spectra;
- There was more debris on the inner surface of Filter 1 than on that for Filter 2;
- Hg was absent from Filter 1 coupons, but was widely dispersed on some Filter 2 coupons;
- The sintered stainless steel filter accounted for the detection of: Fe, Ni, and Cr;
- Common elements detected on the filter coupons include: Al, Hg (Filter 2 only), Na, O, S, Si, and Ti.

For images captured from backscattered electrons (BSD) the underlying metal appears bright, while the debris appears darker colored. For the secondary electron (SE) images it is just the opposite. When reviewing the SEM images of snapped coupon edges, the inside surface of the filter can appear on the right, left, top, or bottom, so it is important to read the image caption closely.

3.4.3.1 Filter 1- Bottom Coupons

In Figure 3-13, the snapped edge of coupon 1BA is shown as both a BSD image (left) and SE image (right). The inner filter edge is on the right. As one can see from examining these two images, there is no noticeable fouling layer on the inner surface of the coupon as compared to the external side, except microscopically, both appear relatively clean. This was a common observation for all the filter coupons examined.

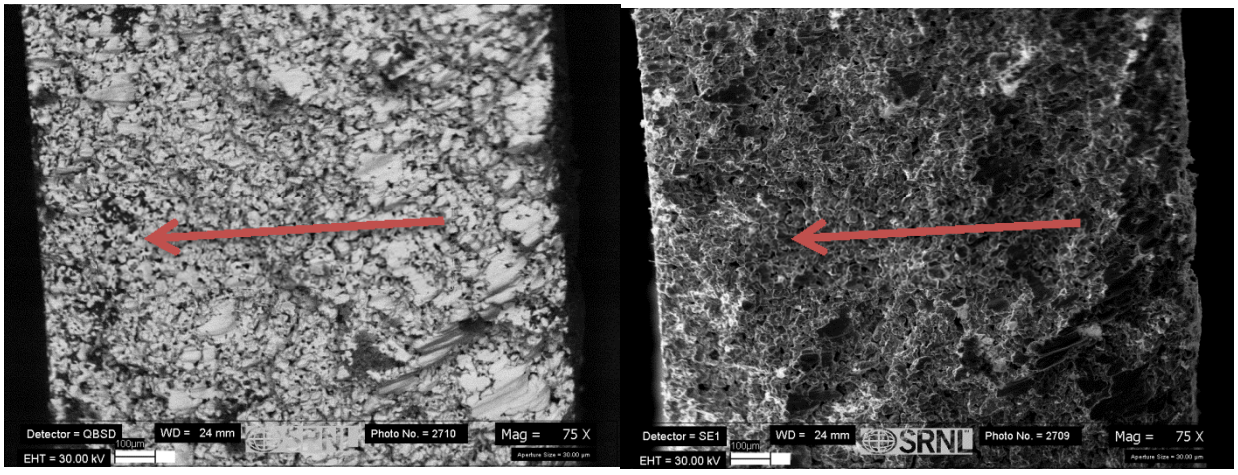

Figure 3-13 Filter 1, Coupon 1BA, SEM Images Showing Snapped Edges with the Inside Surface on the Right Side. The image on the left is from the backscattered electrons (BSD) and the image on the right is from secondary electrons (SE). Flow direction shown with arrow.

In Figure 3-14, the inner surface of coupon 1BB is shown as the BSD image. Deposits on the metal surface appear as dark areas in this picture. It is evident in this image that vast areas of the surface are not covered by deposits, which cover ~30 % of the surface in this image. This was a common observation for all the filter coupons examined.

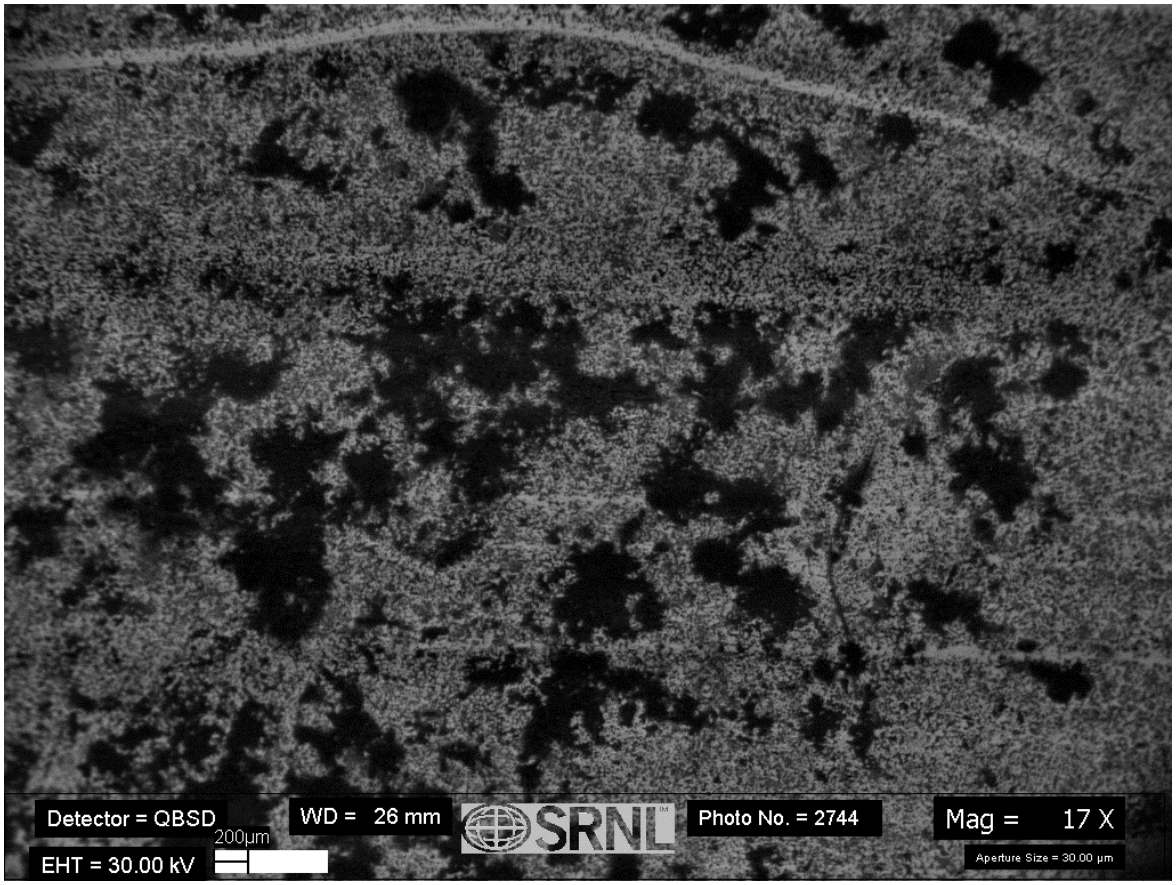

Figure 3-14 Filter 1, Coupon 1BB, SEM Image Showing Surface Deposits (Dark Areas)

The debris layer on the top, inner filter surface of coupon 1BB is clear in Figure 3-15, but the solids are visible on both the inner and outer surface of the snapped edge. The solids do appear to fill in the surface pours of the sintered stainless steel. In Figure 3-16 (the top image is the same as that in the left image in Figure 3-15), the EDS spectra collected on the raster area marked with a "5" gives one of the clearest spectra of the base sintered stainless steel containing Cr, Fe, Mo, and Ni. This pattern will be seen in many of the spectra obtained during the SEM analyses of the coupons. For Filter 2 coupons, it will clearly show the presence of Hg, which is not present on the Filter 1 coupons. The EDS spectra for "4" is the same as that collected for spots 1-3, and indicates that the deposited solids are Na and O containing, hence likely salt deposits of evaporated liquid. Closer examination reveals traces of Al, Ca, Cl, S, Si, and/or Ti containing species on the inner surface along with the sodium containing salt deposits already discussed. As an example, Figure 3-17 provides the EDS spectra for Spot 1 in Image 2758 of coupon 1BB (which corresponds to a spot in the middle of the upper right quadrant of Image 2744 in Figure 3-14) that shows a strong Ti signature. A nearly identical spectra is found for Spot 2, while Spot 3 is the sintered stainless steel.

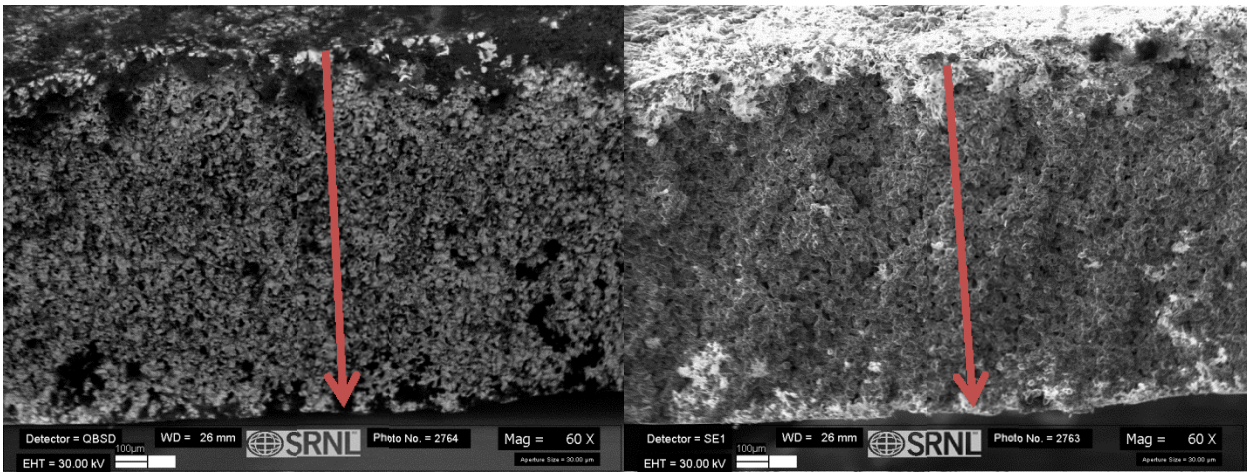

Figure 3-15 Filter 1, Coupon 1BB, SEM Image Showing Snapped Edges with the Inside Surface on the Top. The image on the left is from the backscattered electrons (BSD) and the image on the right is from secondary electrons (SE).

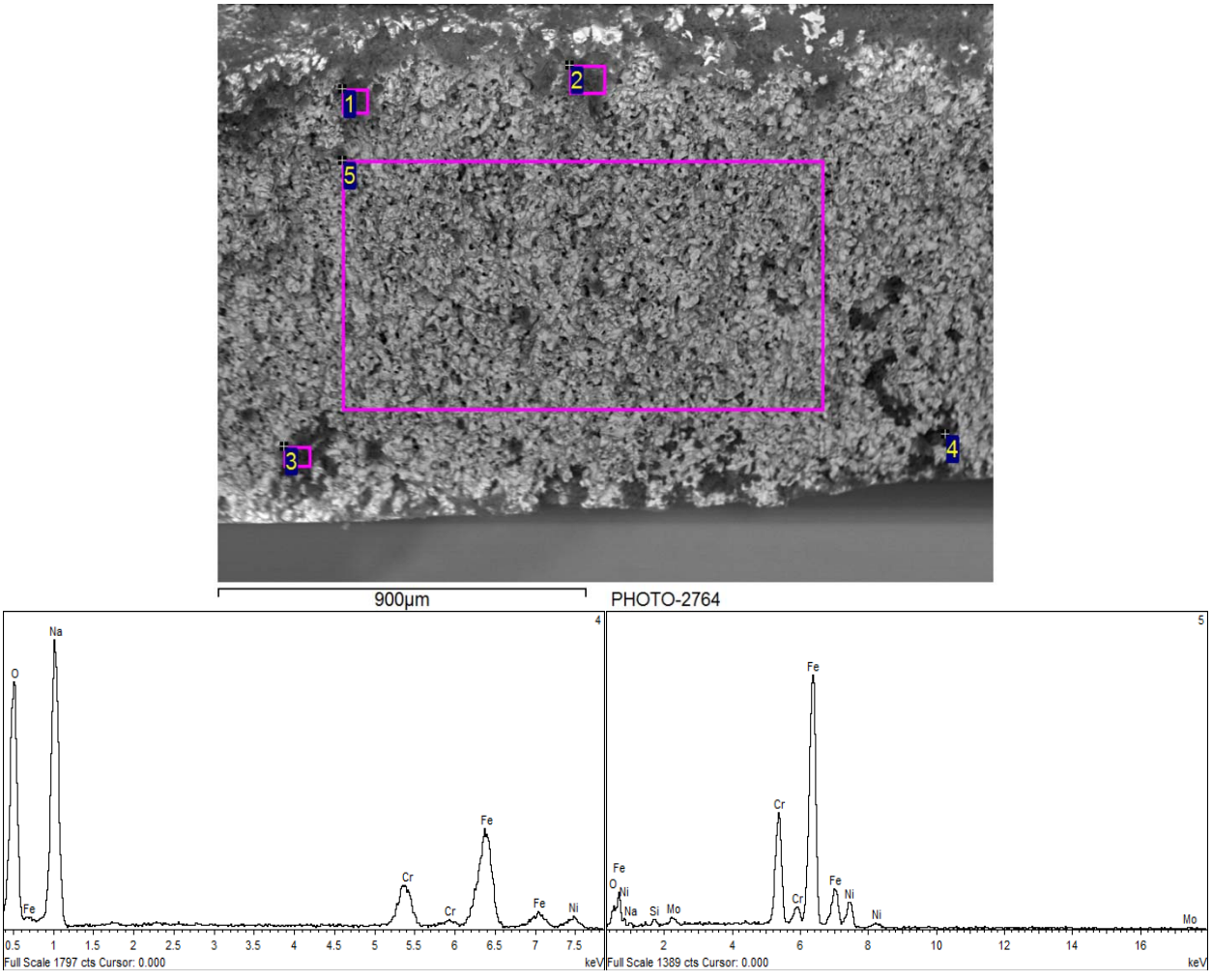

Figure 3-16 Filter 1, Coupon 1BB, Image 2764 and EDS Spectra for Spot 4 (Left) and 5 (Right)

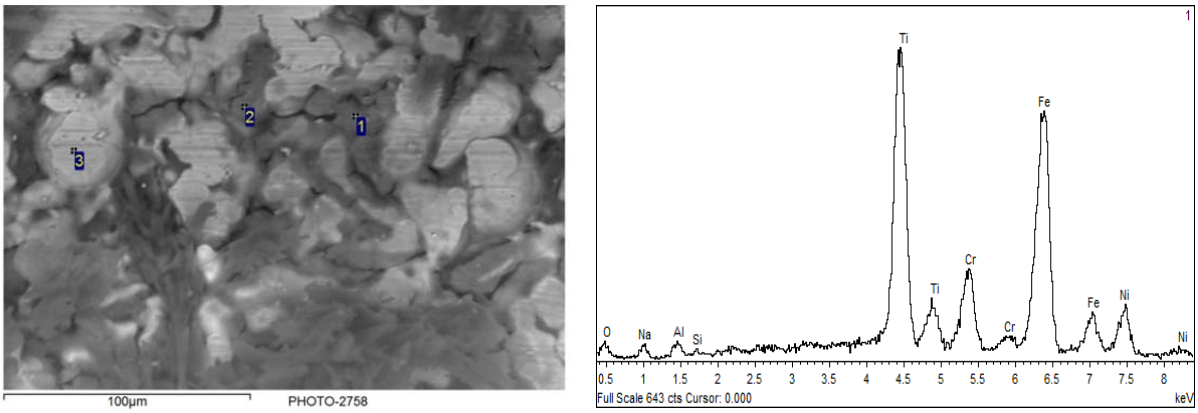

Figure 3-17 Filter 1, Coupon 1BB, Image 2758 and EDS Spectra of Ti Deposits (Spots 1 & 2)

3.4.3.2 Filter 1 – Top Coupons

During examination of the top coupons from Filter 1, specifically Coupon 1TA, there were spots with strong, nearly Al-only spectral signatures. Figure 3-18 shows Spot 2 on the inside surface of Coupon 1TA that is high in Al and gave a signal well above that of the background sintered stainless steel. It is difficult to say for certain if this is a deposit or debris collected during handling, though similar Al deposits were observed on other coupons. Hobbs[17] has noted that metal loading by titanate materials is higher for trivalent metal ions than for divalent ions in weakly acid solutions, but in caustic solutions Al is present as a variety of polymeric hydroxy anion species, so it is unclear why these concentrated Al deposits are observed here unless they were deposited during washing operations and left behind on the filter.[18]

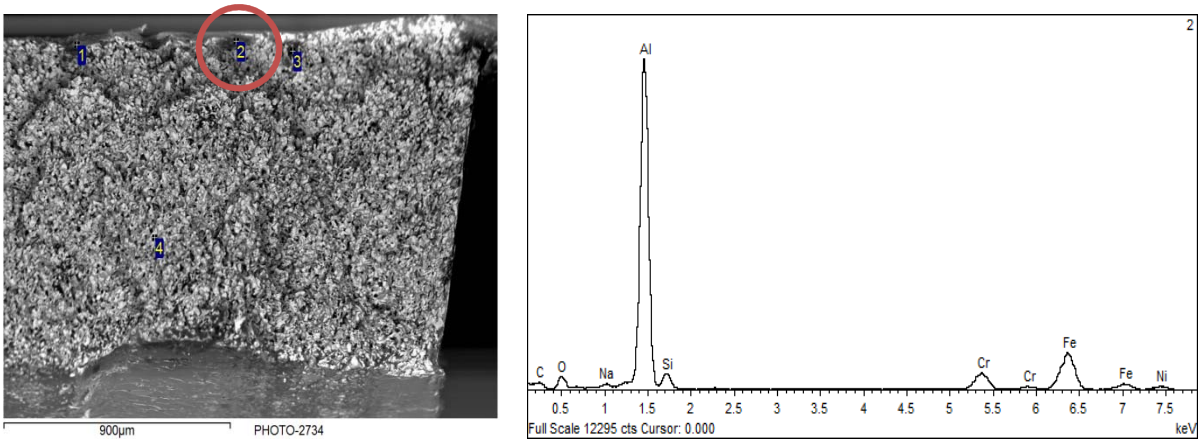

Figure 3-18 Filter 1, Coupon 1TA, Image 2734 and EDS Spectra of Al Deposits (Spot 2)

Figure 3-19 provides an image from Coupon 1TB along with the selected regions for EDS spectral analysis. The spectra obtained provide an example of how complex the deposits can be when they are examined closely. Aside from the typical sintered stainless steel signal for Cr/Fe/Ni seen in the 5.4 – 7.5 keV region, Raster Area 1 in Figure 3-20 in addition to strong signals for Na and O, shows strong signals for Al, Ca, Cl, and Si, in addition to weaker signals from Cl, Mg, P, and S. The spectra obtained for Raster Area 2 (not shown) was similar with a slightly stronger Fe and Ti signals. Raster Area 3 (not shown) is similar to Raster Area 4's spectra in Figure 3-20 with a stronger Ti signal and weaker contributions from Al, S, and Si.

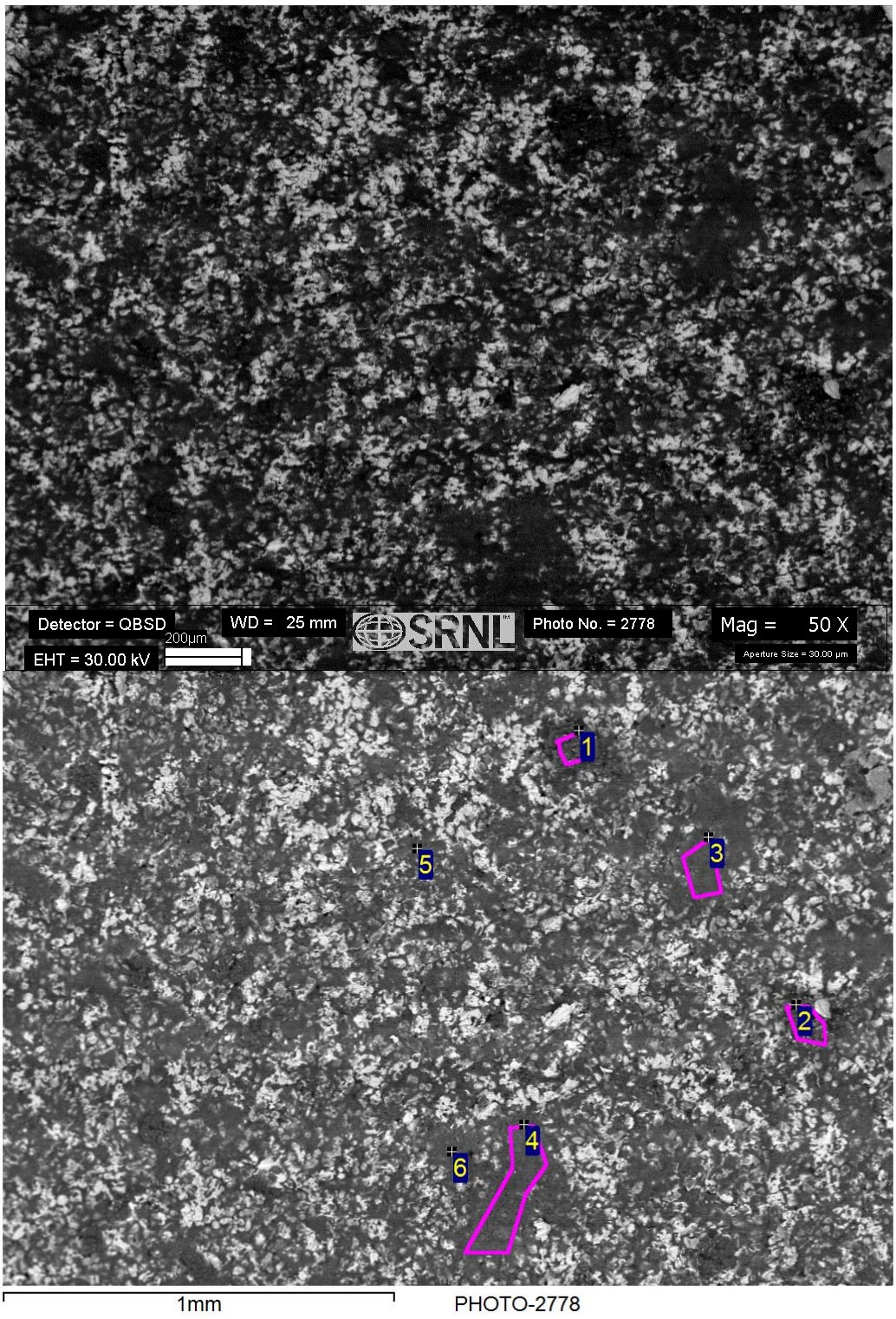

Figure 3-19 Filter 1, Coupon 1TB, SEM Image 2778 showing regions selected for EDS spectral analysis

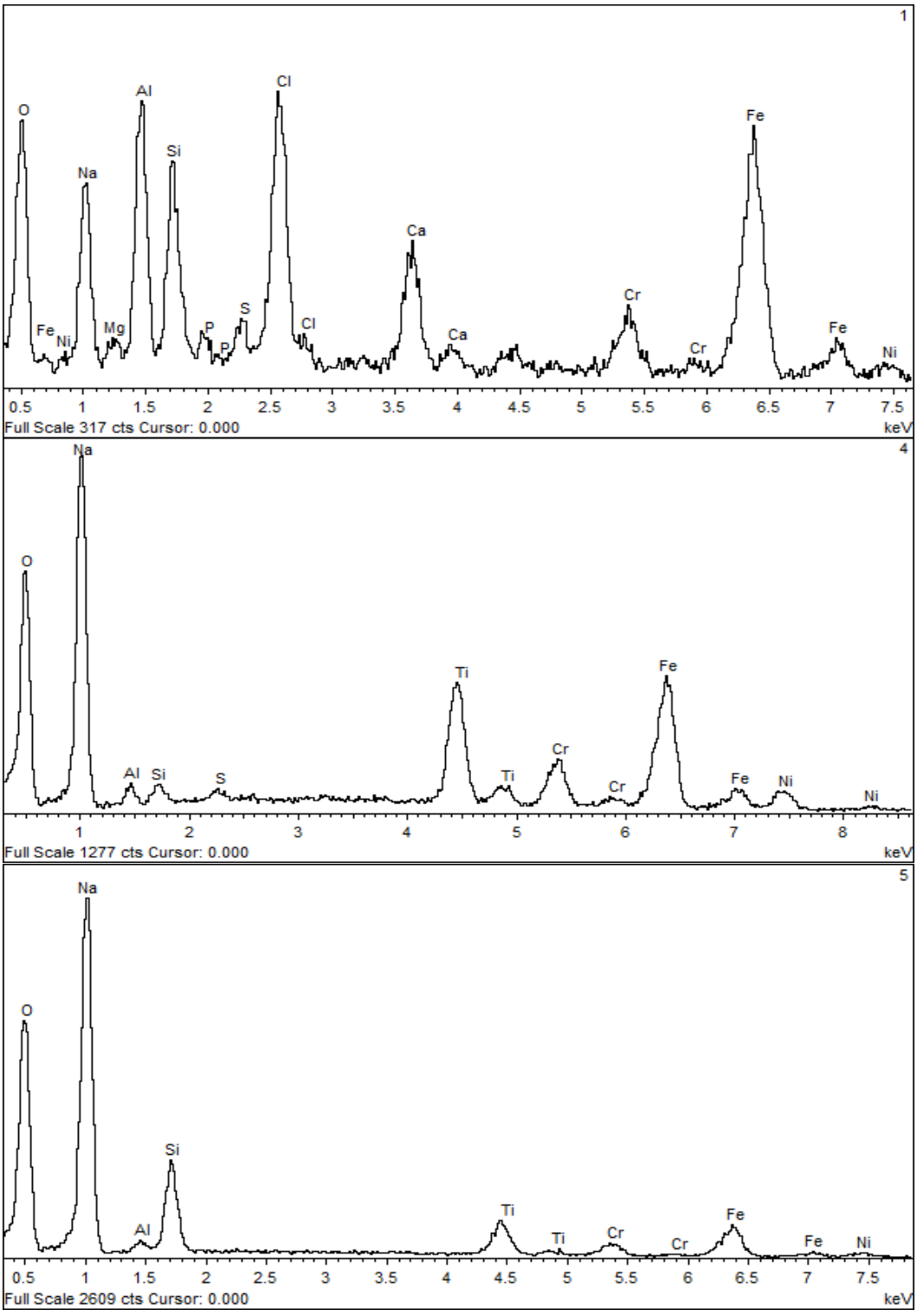

Figure 3-20 Filter 1, Coupon 1TB, Image 2778, EDS Spectra for Raster Areas 1 & 4, and Spot 5

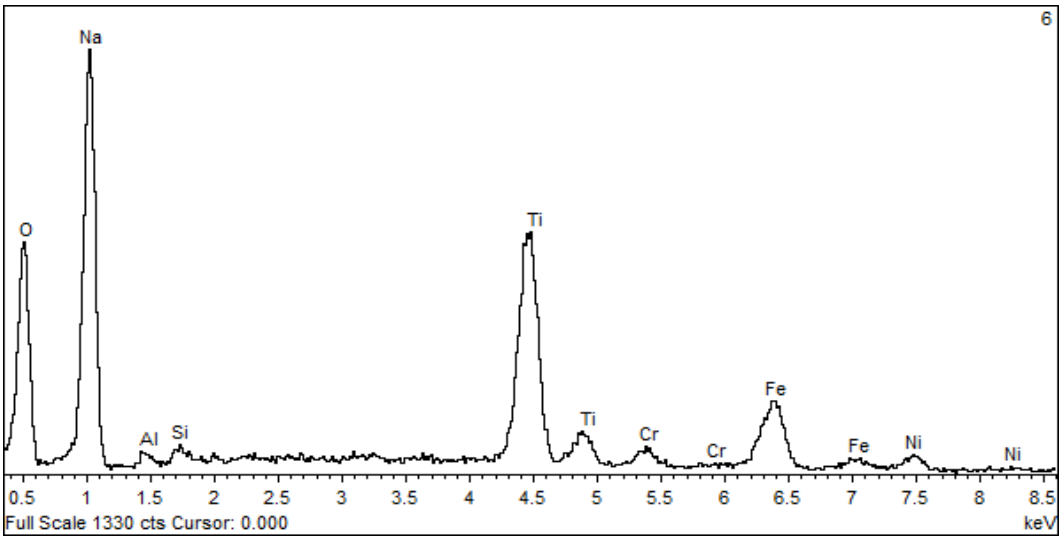

Figure 3-21 Filter 1, Coupon 1TB, Image 2778, Spot 6 EDS Spectra

Spot 5's spectra in Figure 3-20 shows a strong Si signal and weaker contributions from Al and Ti, while Spot 6's spectra shown in Figure 3-21 has a strong Ti signal and weaker contributions from Al and S. The deposits on Filter 1 while not extensive, are varied and probably represent deposits of aluminosilicates, aluminum hydroxides, silica, titanium compounds including MST, and various sulfates and chlorides in addition to sodium salts of nitrates and nitrites. The salts were probably deposited during drying, but the insoluble species probably represent fines that made it through the primary filter, but became lodged in the secondary filter.

3.4.3.3 Filter 2 – Bottom Coupons

The SEM-EDS results for the Filter 2 coupon analyses are not unlike those obtained for Filter 1. The image in Figure 3-22 shows the typical collection of dark solids on the brighter white sintered stainless steel surface of Coupon 2BA. Some of the solids appear as a powdery looking solids while other deposits are needle-like crystals. The item that is unique in Filter 2 as compared to Filter 1 was the presence of Hg, which was first noticed during an examination of a raster area of deposited solids on coupon 2BA. Figure 3-23 shows Raster Area 2 and the spectra indicating the presence of Hg with its characteristic signals at 2.2, 10, and 11.8 keV.

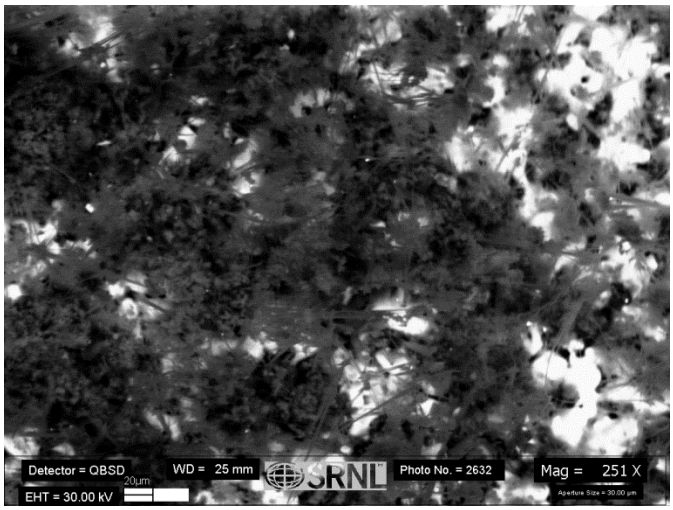

Figure 3-22 Filter 2, Coupon 2BA, SEM Image 2632

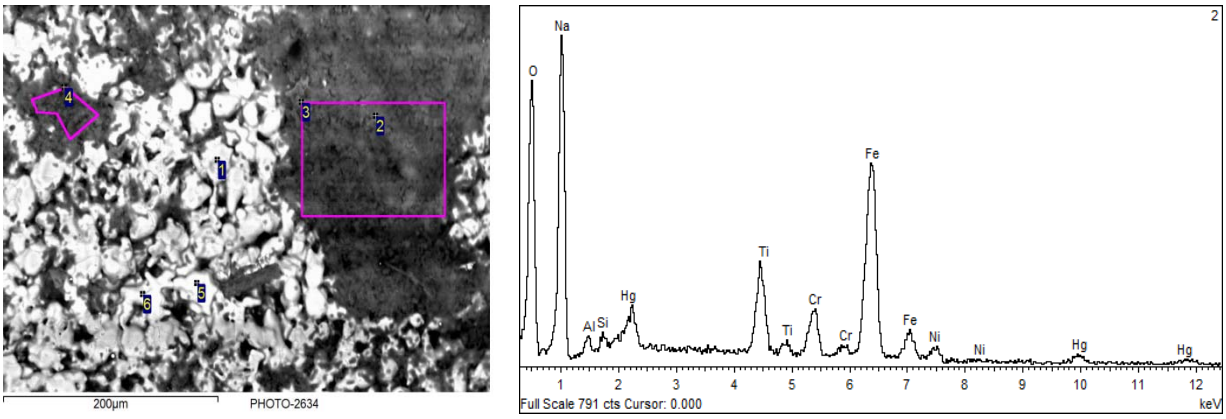

Figure 3-23 Filter 2, Coupon 2BA, SEM Image 2634 and EDS spectra for Raster Area 2

The presence of Hg was also detected on Coupon 2BB and the spectra for Spot 1 of Image 2840 in Figure 3-24 shows a very clear spectral signature for the element with the only other significant contribution coming from Na and O.

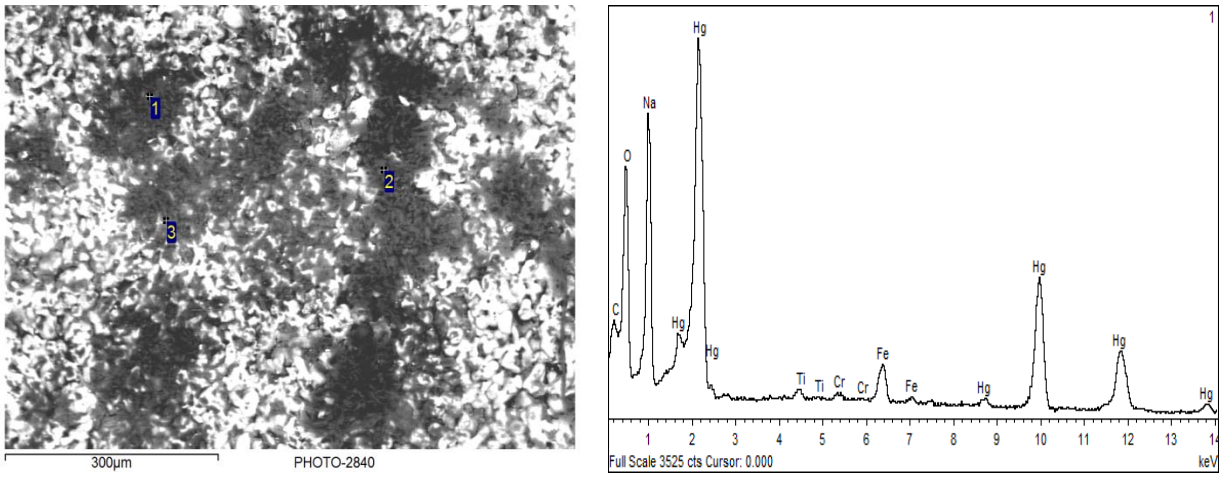

Figure 3-24 Filter 2, Coupon 2BB, SEM Image 2840 and EDS spectra for Spot 1

3.4.3.4 Filter 2 – Top Coupons

On the top coupons of Filter 2, the Hg compound(s) are visible as distinctive bright white spots scattered across the surface of the sintered stainless steel. Image 2810 in Figure 3-25 and the spectra obtained in Figure 3-26 for the largest of the white spots in Image 2810 clearly displays this phenomenon. The dark areas between the sintered metal surface (medium gray color) are comprised of Al, Si, and Ti in varying proportions depending upon the specific area examined. The Hg appeared to be confined to the inner surface of the coupons, whereas other elements, such as Na, Al, S, and Ti, appear to migrate into the sintered metal surface. This migration is evident when the snapped edges are examined.

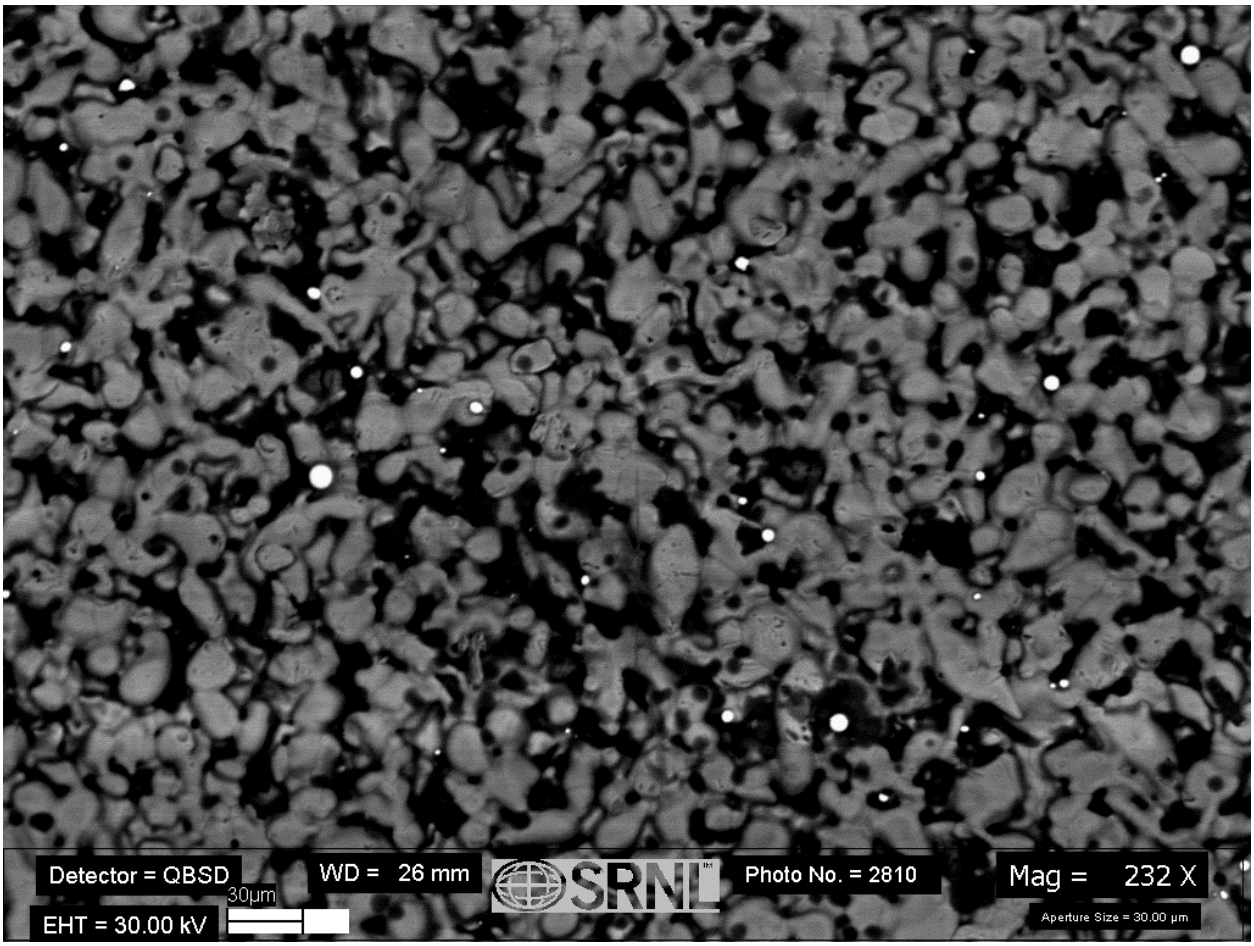

Figure 3-25 Filter 2, Coupon 2TA, SEM Image 2810 showing Hg beadlets

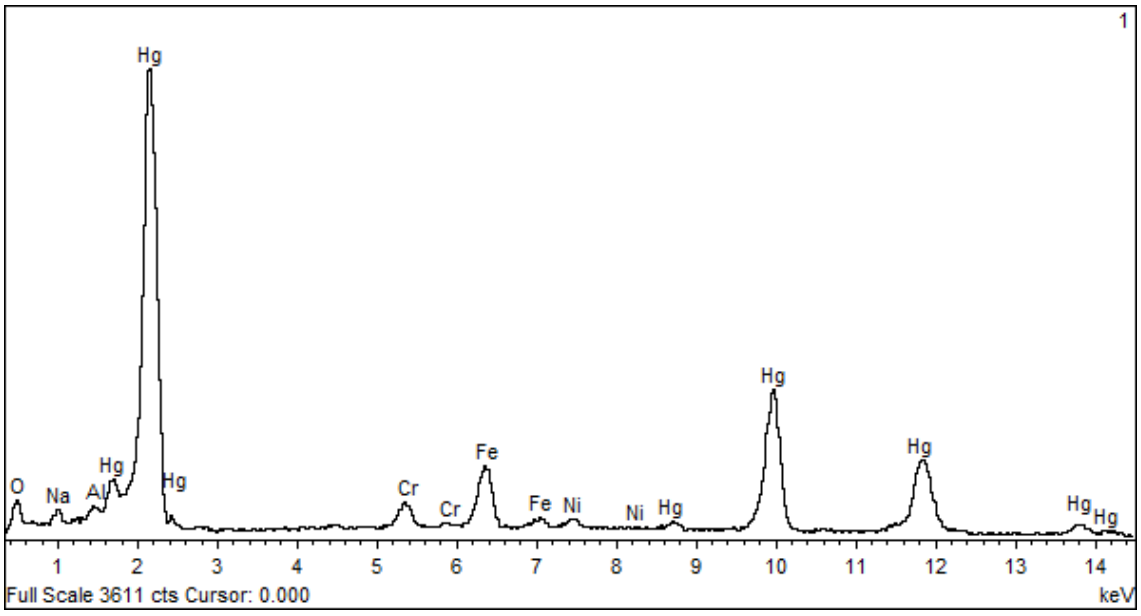

Figure 3-26 Filter 2, Coupon 2TA, EDS Spectra for the largest white spot in Image 2810 (Figure 3-25)

Figure 3-27 shows Spots 1, 2, 4, and 5 examined near the outer surface edge of the snapped coupon 2TA. The spectra indicate Na and O, likely from salt deposits, but also Al, S, and Ti, but no Hg – these spectra are not included in this report. Spot 3, well through the filter media gave a surprisingly clean spectra for Al which is shown in Figure 3-28.

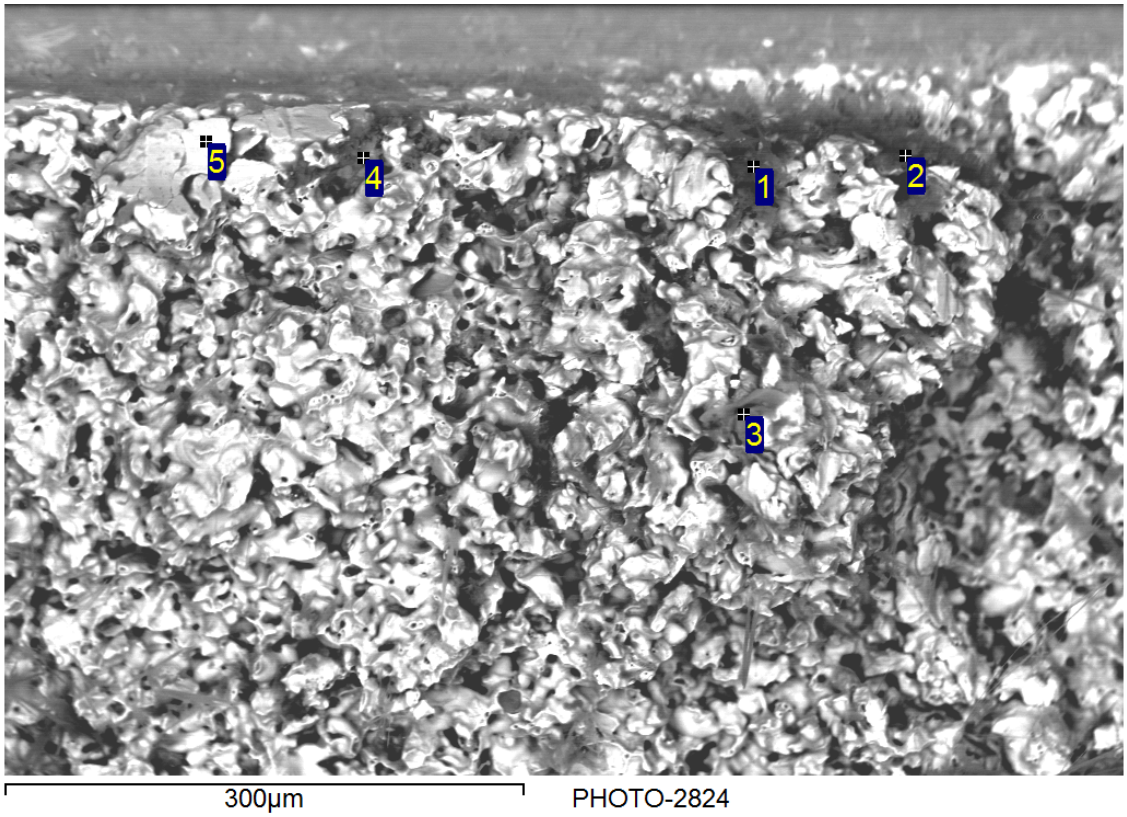

Figure 3-27 Filter 2, Coupon 2TA, Image 2824 showing numbered areas examined on the outer surface of the snapped edge of the coupon

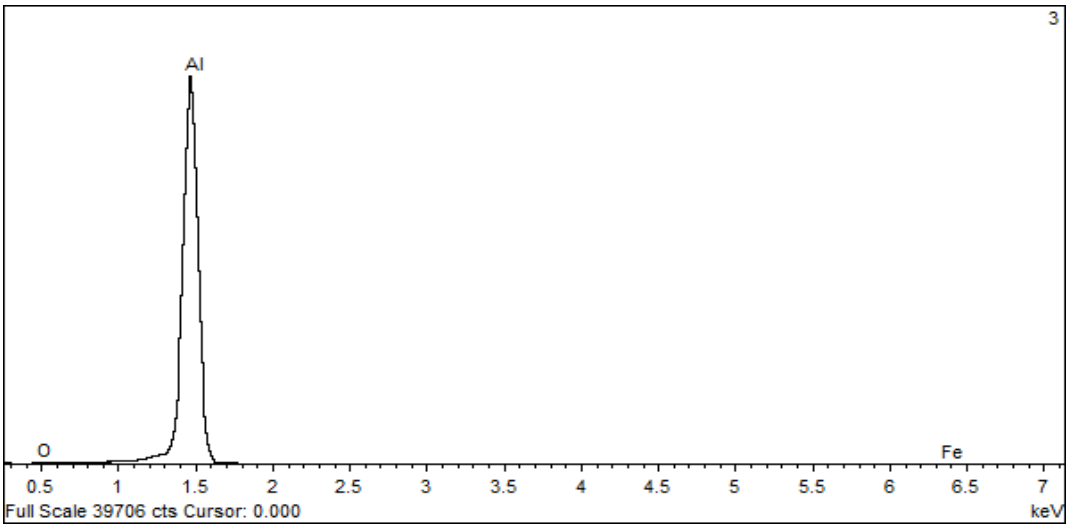

Figure 3-28 EDS Spectra Filter 2, Coupon 2TA, Image 2824 for Spot 3

The images and spectra obtained for the final coupon, 2TB, were similar to features and observations gathered from the other seven coupons. There was one unusual feature, that should not be over interpreted since it likely represents cross contamination introduced during handling. The SEM image and spectra showed a spot midway through the snapped edge containing a strong signal for Cu at 0.9, 8.0, and 8.9 keV as well as a weak signal for Mg, along with the now commonly expected signals from O, Al, Si, S, Cl, Ca, Cr, Fe, and Ni. It was also unusual that the Cl signal was so strong at this location since previous Cl signals had been relatively weak. The SEM Image 2870 showing the placement of Spot 2 and the spectra obtained for it are given in Figure 3-29.

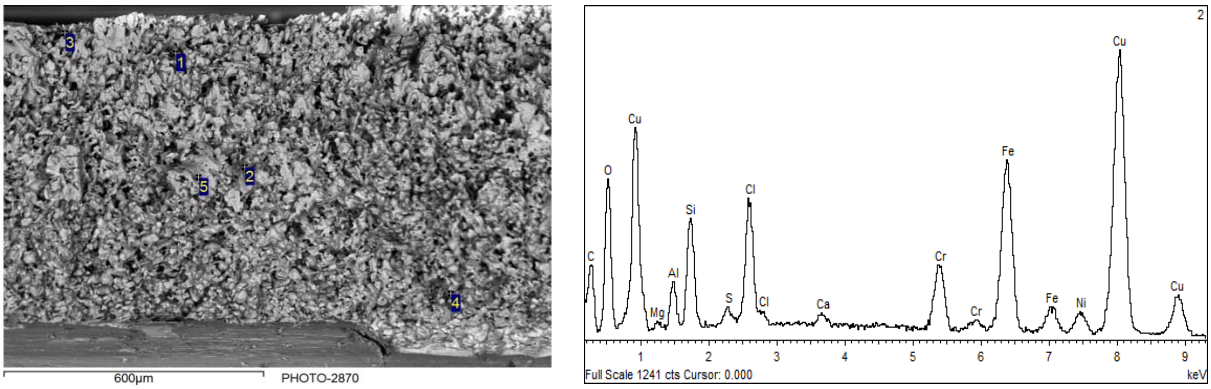

Figure 3-29 Filter 2, Coupon 2TB, SEM Image 2870 and EDS Spectra Showing Cu

3.4.3.5 Tank 50 Hg Levels

The level of soluble Hg in Tank 50 has been increasing over time based upon the measurement of Hg conducted on the quarterly Waste Acceptance Criterial (WAC) samples from this tank.[i] The trend for successive Salt Batches (SaB) based on the blend calculations for Tank 49 has seen similar increases for SaB1, SaB2, SaB3, SaB4b, SaB6d and SaB7b,[19, 20, 21, 22, 23] the latest Salt Batch that has been processed as of this writing. Note that no blend evaluation for Tank 49 was available for SaB5 The value determined for SaB8 is 129 mg/L shows a further increase in soluble Hg and should further increase the blend calculated value for Tank 49. Shown in
Figure 3-30 is a plot of Hg over time for Tank 50 and Tank 49 (Salt Batches 1, 2, 3, 4b, 6d, and 7b). The upward trend since 2008 is readily apparent.

[i] See each Quarterly Tank 50 WAC report for this Hg data, the 26 reports are not referenced individually in this document.

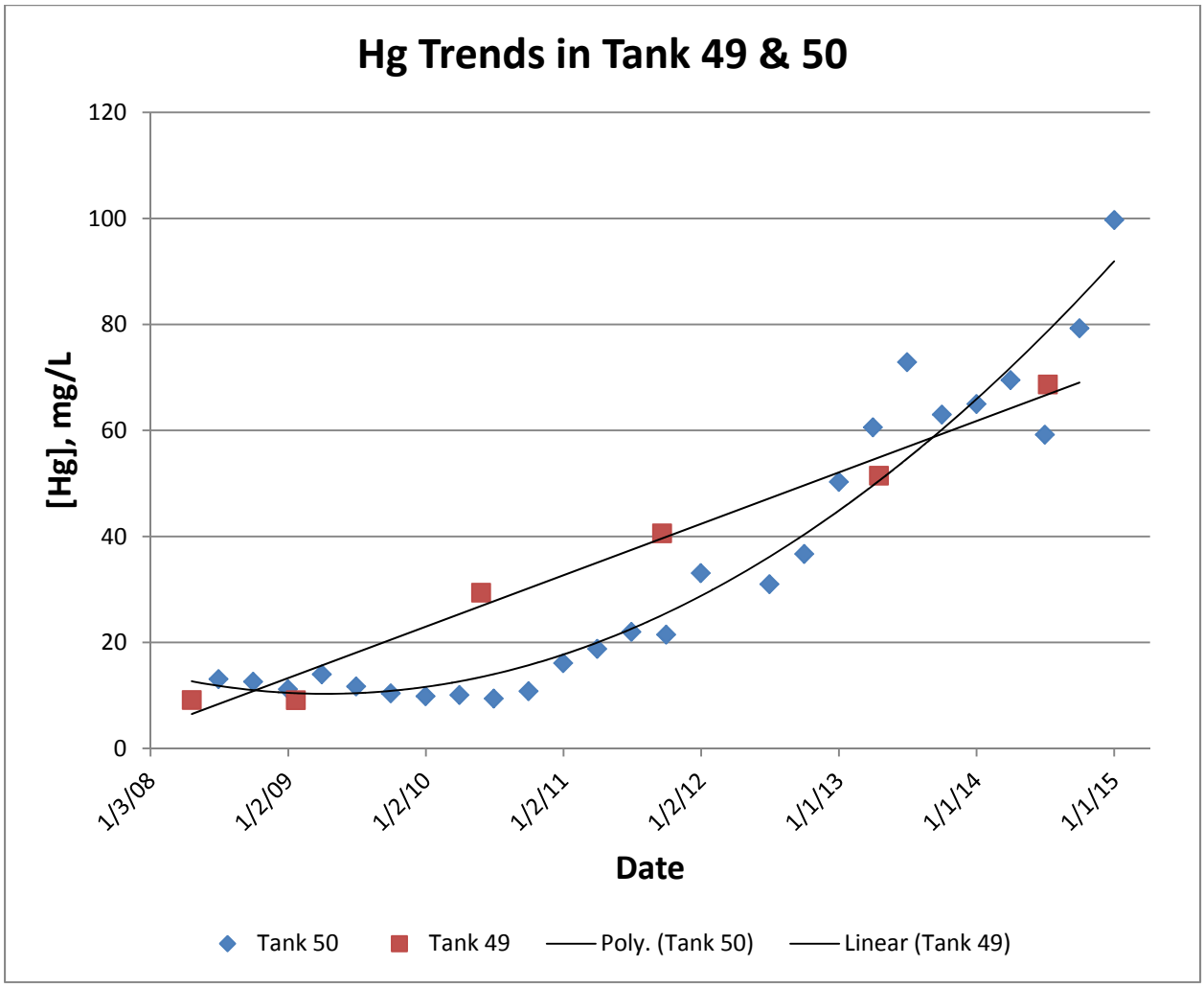

Figure 3-30 Concentration of Hg in Quarterly Tank 50 WAC Samples and Tank 49 (Salt Batches 1, 2, 3, 4b, 6d, and 7b)

A major Hg source term for Tank 50 is the ARP/MCU stream so it would appear that Hg is getting through the primary filter to the secondary filter and beyond, ending in Tank 50 where it may now be reaching its solubility limit in caustic. According to alkaline low-activity waste (LAW) data from Hobbs[24], the solubility of Hg reaches a maximum of 90 mg/L at 1.2M OH^-. His data was consistent with literature data which reported a Hg solubility (measured as HgO, but given here in terms of Hg) between 46 mg/L to 65 mg/L in 0.01M to 2.1M NaOH.[25] Figure 3-31 shows the variation in Hg concentration as a function of free OH^- concentration in Tank 50 Quarterly WAC samples. The maximum [Hg] measured was 73 mg/L at 1.9M [OH^-] in the 3Q13 sample.[26] Any additional Hg above the solubility limit would likely be in the settled solids.

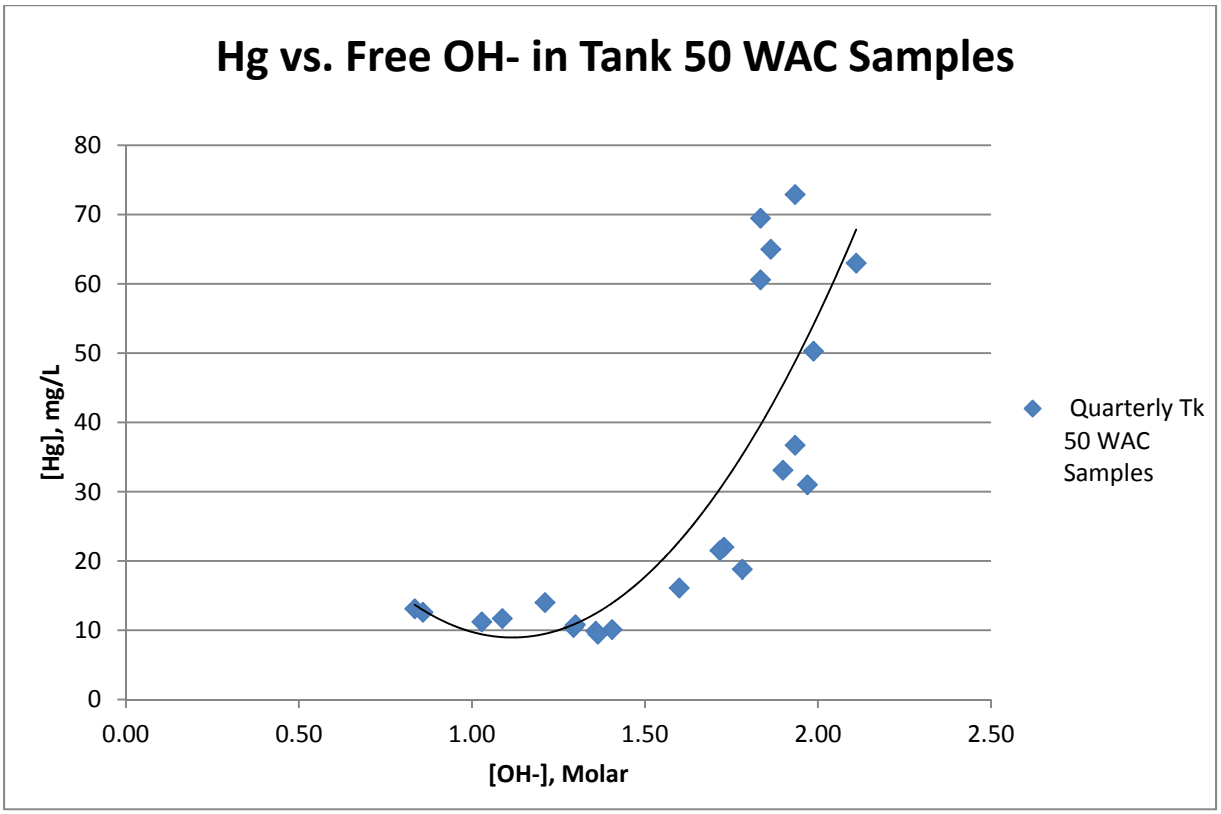

Figure 3-31 Variation in Hg Solubility vs. Free [OH^-] in Tank 50 WAC Samples

3.4.4 FTIR

FTIR analysis was done on a series of Filter 1 coupons: 1BE, 1BF, 1BG, 1TE, 1TF, and 1TG; as well as Filter 2 coupons: 2BE, 2BF, 2BG, and 2TE. The general observation was that the deposits showed nitrates, nitrites, and carbonates (red trace in Figure 3-32), but upon removal of the top layer of salts, the signatures of additional organic species were evident (blue trace in Figure 3-32).

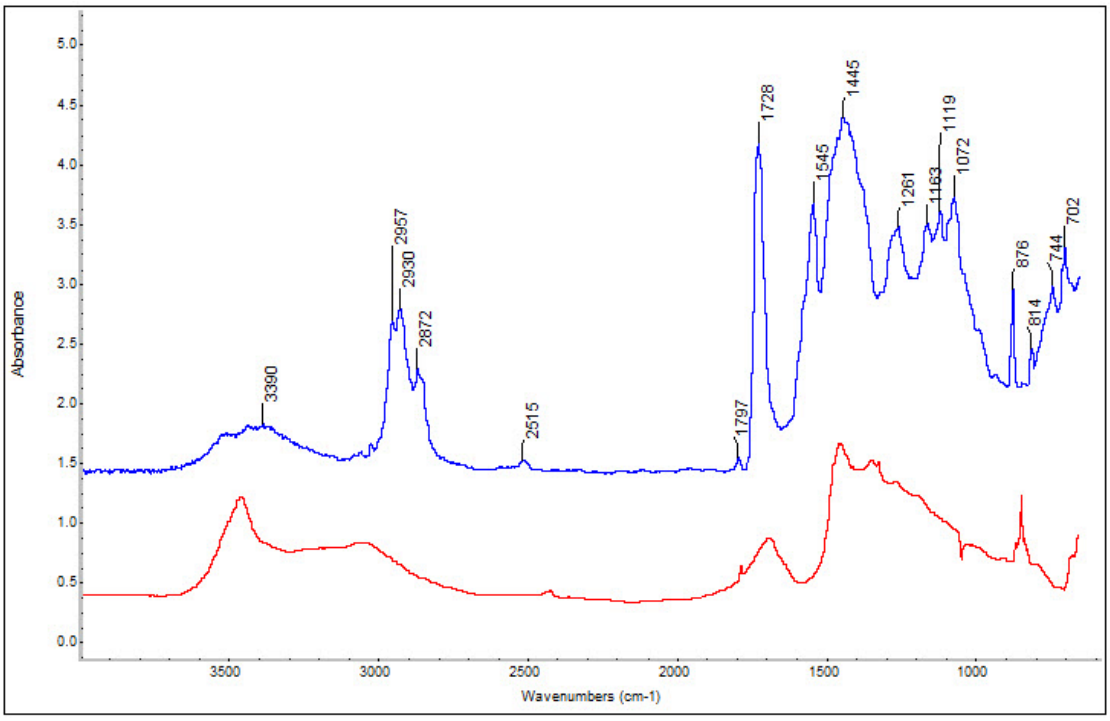

Figure 3-32 Filter 1 FTIR Spectra. Red trace is the as-received analysis. Blue trace is after removal of the top layer of salt deposits.

The organic layer had a "pinkish" tone to the solids. The organic material appeared to be an ester containing acetate and possible sulfone. A sulfone has the general formula R-S(=O)$_2$-R', where R and R' are organic groups. As shown in Figure 3-33, "R" may be the same or different organic chains. Sulfones can be the oxidation product of sulfides and sulfoxides, and some polymers contain sulfone groups.

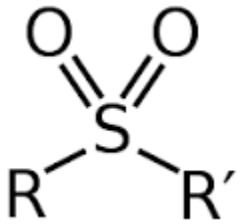

Figure 3-33 Sulfone General Formula

The data obtained from specific Filter 1 coupons will be presented first, and then that obtained for Filter 2 coupons.

3.4.4.1 Filter 1

The bottom coupons collected from Filter 1 provided the following FTIR spectral data. Figure 3-34 provides the two FTIR spectra obtained for coupon 1BE. The blue trace represents the majority of the material on the coupon and is comprised of a mixture of nitrates, nitrites, carbonates, and some nitriles. After removing the top layer of salts, the underlying material provided the spectra shown in red. The evidence of a possible alkyne is the C-H stretch at 2921 cm^{-1} along with the potential C≡C-H stretch at 3398 cm^{-1}, though this is by no means conclusive.

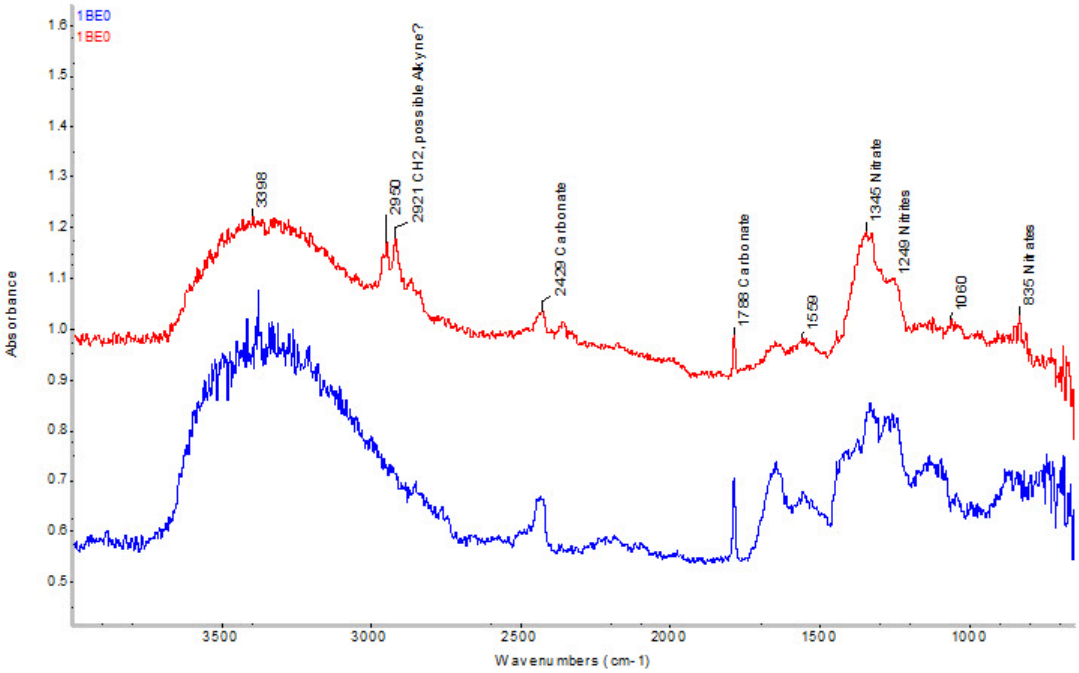

Figure 3-34 FTIR Spectra for Filter 1, Coupon 1BE

Spectral traces obtained from examination of coupon 1BE are shown in Figure 3-35. The red trace indicates carbonate containing materials due to the absorbance values at ~800, 1466, and 1789 cm^{-1}. The purple trace represents the majority of the material found on the coupon: nitrates, nitrites, and carbonates. Nitrate absorbance is seen as the left peak of the double peak at ~800 cm^{-1} and also 1367 cm^{-1}, while the right peak at ~800 cm^{-1} corresponds to a carbonate absorbance. The nitrite absorbance is at 1262 cm^{-1}.

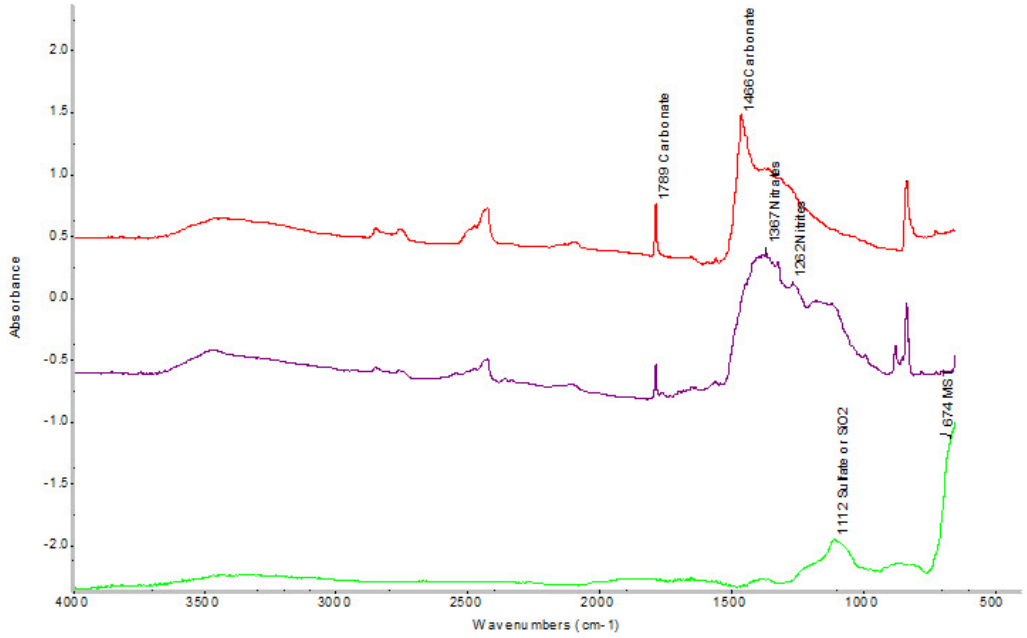

Figure 3-35 FTIR Spectra for Filter 1, Coupon 1BF

The green trace in Figure 3-35 provides evidence for sulfates on the coupon surface due to the absorbance at 1112 cm^{-1}, while evidence for the presence of MST is seen by the absorption at 674 cm^{-1}.

Figure 3-36 provides a typical spectra for coupon 1BG material comprised of nitrates, nitrites, and carbonates. This coupon's deposits were not examined below the surface material comprised of these salts.

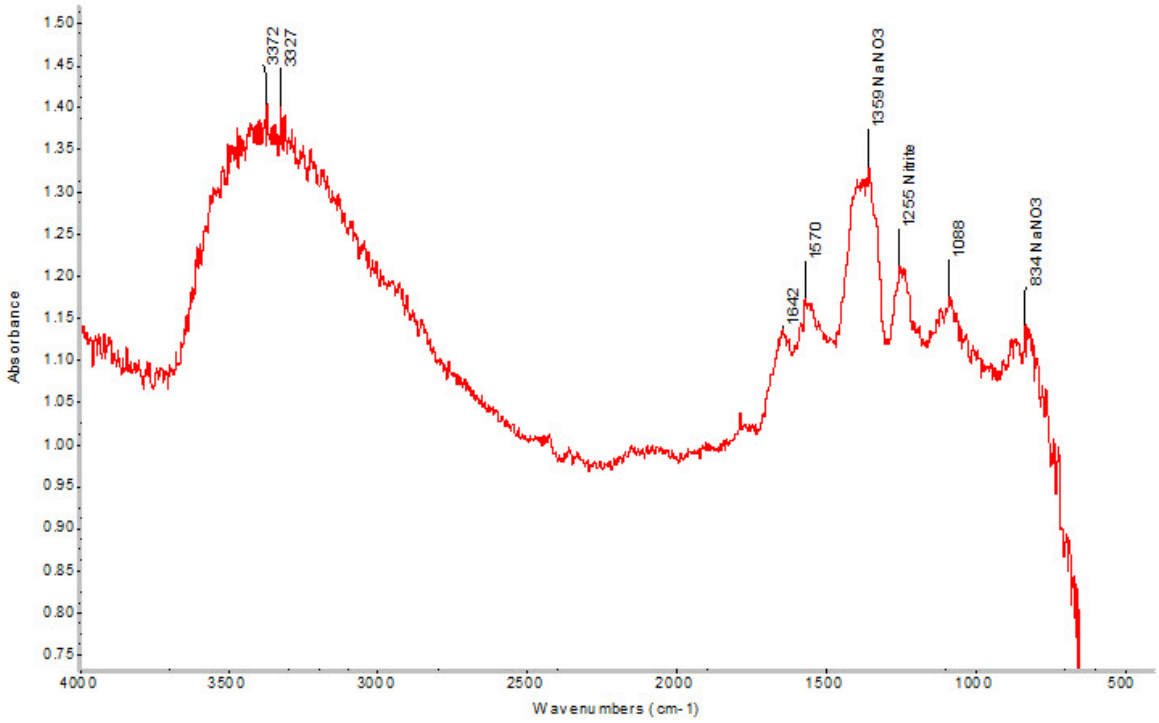

Figure 3-36 FTIR Spectrum for Filter 1, Coupon 1BG

Figure 3-37 provides six FTIR spectra obtained for coupon 1TE. The top four spectra (from the top: teal, dark blue, pink, and gold) show the typical nitrates, nitrites, and carbonates. These salts may comprise a variety of different compounds depending upon whether the cation is an alkali metal ion, alkaline earth metal ion, or a transition metal ion.

Removing the top surface of material from the coupon yields material with the spectra shown in green that contains an ester as evidenced by the C-H stretch around 2900 cm^{-1}, the C=O stretch at 1723 cm^{-1}, and C-O stretch around 1050 cm^{-1}. Esters have the general formula, R-(C=O)-O-R'.

Another material found in the layer below the salts is an amide characterized by the N-H stretch at 3288 cm^{-1}, the C=O stretch at 1634 cm^{-1}, the N-H bend at 1520 cm^{-1}, and the N-H bend overtone absorption at 3063 cm^{-1}. Amides have the general formula R-(C=O)-NHR'.

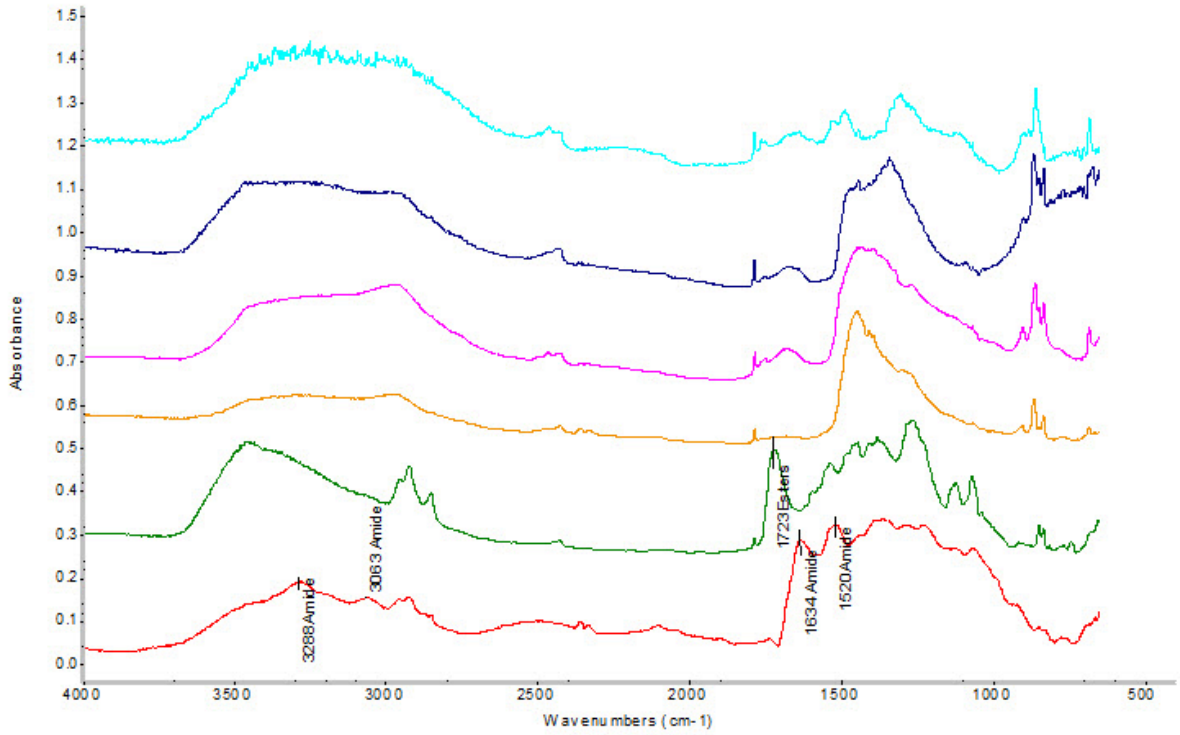

Figure 3-37 FTIR Spectra for Filter 1, Coupon 1TE

3.4.4.2 Filter 2

All the spots analyzed on Filter 2, Coupon 2BE (Figure 3-38) indicated a mixture of carbonate, nitrates, and nitrides of the alkali and alkaline earth metals. A similar situation existed for the examination of Coupon 2BF that in addition to the carbonates, nitrates, and nitrites, also indicated the presence of sulfates at 1150 cm^{-1} as shown in Figure 3-39 and Figure 3-40. The noise in the latter spectra is due to sulfate scattering. Only one top coupon was examined for Filter 2 and these spectra are shown in Figure 3-41. The red spectra for Coupon 2TE shows a weak C-H stretch at 2906 cm^{-1}.

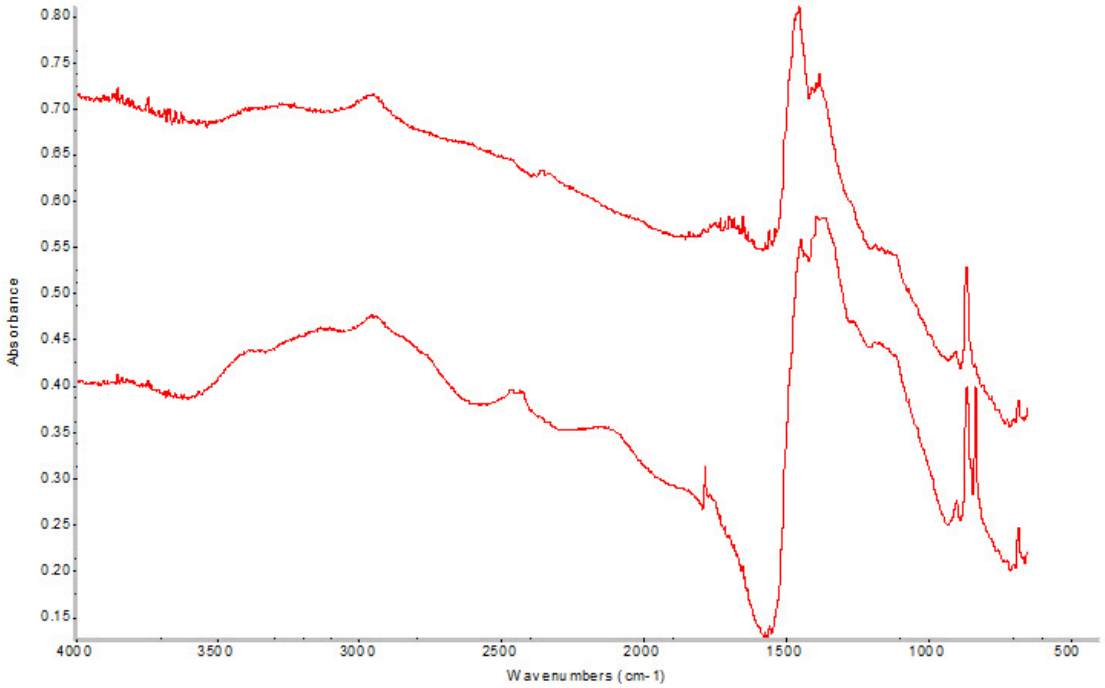

Figure 3-38 FTIR Spectra of Filter 2, Coupon 2BE

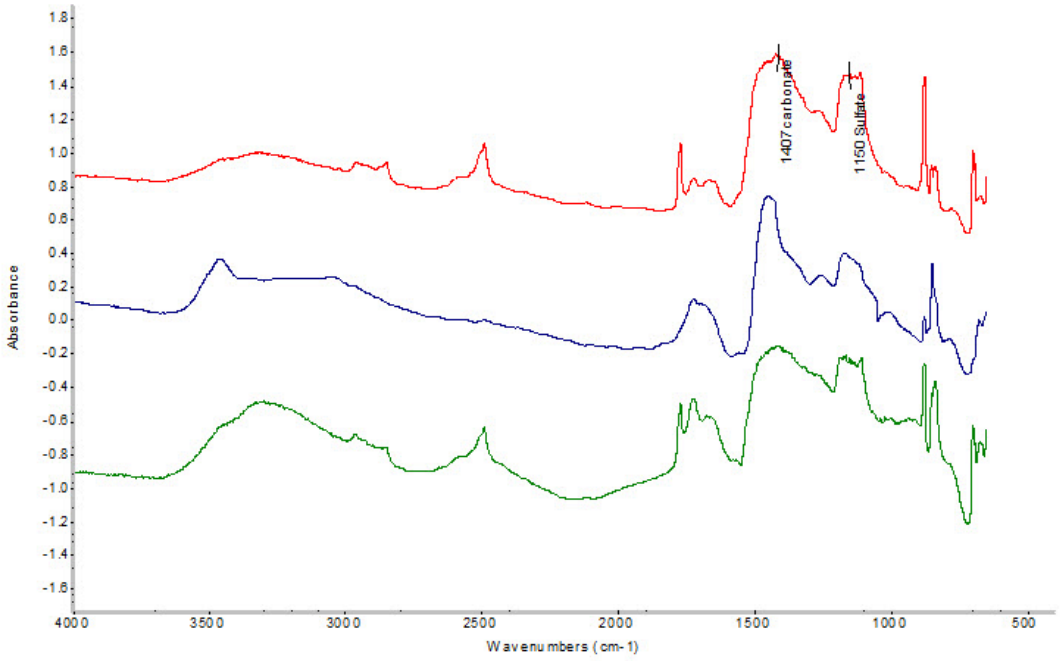

Figure 3-39 FTIR Spectra of Filter 2, Coupon 2BF

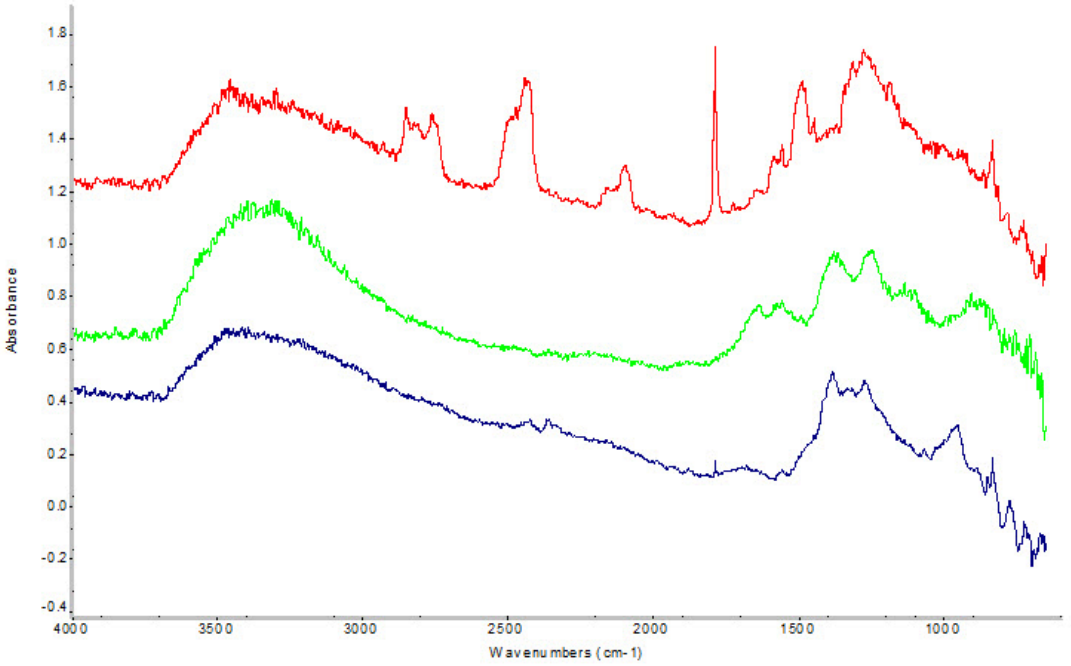

Figure 3-40 FTIR Spectra of Filter 2, Coupon 2BG

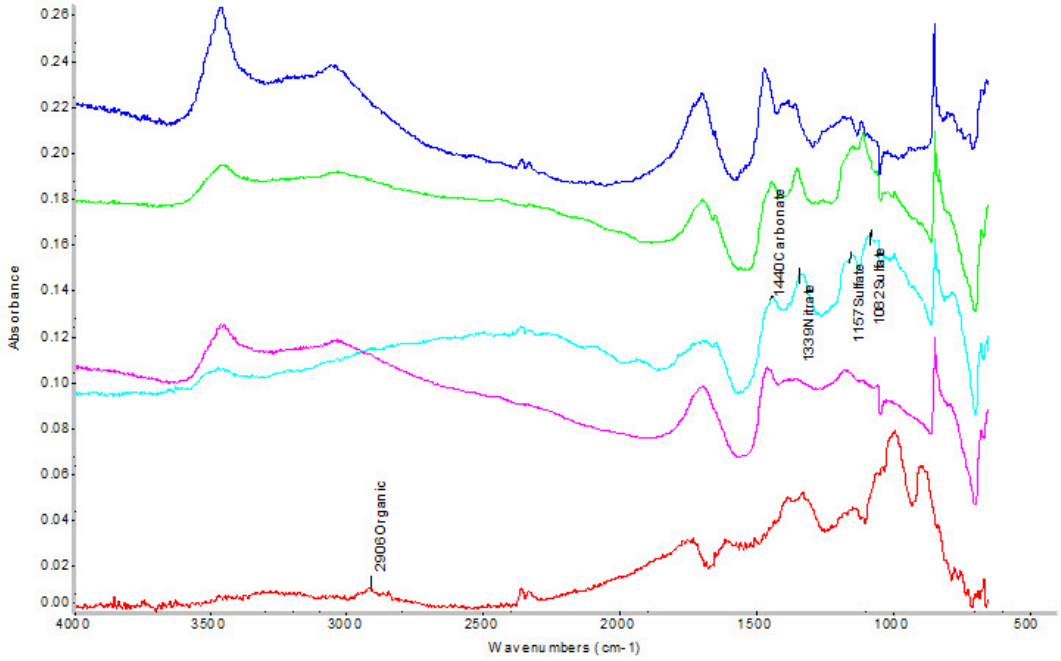

Figure 3-41 FTIR Spectra of Filter 2, Coupon 2TE

3.4.4.3 Comparison of Filter 1 and 2 FTIR Data

The FTIR spectral results for Filter 1 and 2 indicate the presence of a mixture of carbonate, nitrates, and nitrides of the alkali and alkaline earth metals on the surface of the coupons. Some sulfates were also found on both filters. Removal of the salt layer revealed some trace organic constituents in both filters, though more of these trace constituents were observed on the Filter 1 coupons. The source(s) of the organic constituents is unclear but could represent trace organic materials that have found their way into the waste stream from degraded plastics. Some MST was found on Filter 1, but it was not reported in the examination of Filter 2 by FTIR, it may have been removed when the filter was rinsed.

4.0 Conclusions

The 512-S secondary filters received by SRNL did not show major fouling upon visual examination. Closer inspection indicated evidence of aluminosilicates, aluminum hydroxides, silica, MST, and various sulfates and chlorides in addition to various salts of nitrates, nitrites, carbonates. Filter 2 contained Hg, possibly elemental, that was not observed on Filter 1. SEM examination indicated more solids on Filter 1 than Filter 2, which is consistent with it having not been rinsed. The solids that are present appear to be fines that made it through the primary filter and became lodged in the secondary filter. There is some evidence these fines are penetrating into the sintered metal surface and possibly working their way through the secondary filter. It may be these lodged fines that are resulting in the increased pressure drop across the secondary filter.

Comparing the current findings with the 2009 secondary filter analyzed in SRNL[7] we find the following:

1. There was no $CO_{2(g)}$ generation observed during acid leaching of the coupons which is consistent with the lower amount of carbonate salt deposits observed on these filters.
2. MST was not observed on the current filters when examined by XRD as it was in 2009, and only a trace was found by FTIR, though the SEM-EDS analysis, XRF analysis, and acid-leached coupons examined by ICP-AES indicate its presence (measured as Ti) on the filters.
3. Sr-90 is once again the largest contributor to the dose amongst the analyzed radionuclides, but it is difficult to compare activities with the 2009 filter since the earlier leach results were not expressed in units of filter area.
4. Oxalate was the least abundant anion measured while it was the most abundant in the 2009 study.
5. After Na (from salts) and Fe (leached from the stainless steel), Ti was the most abundant metal ion observed in the leachates, and once again its most likely source term is MST fines that made it through the primary filter.

If Hg is present on the primary filter, as it would be expected to be if the primary filter is the source term for the Hg observed in the secondary Filter 2, oxalic acid cleaning may not be suitable. Both HgC_2O_4 and $Hg_2C_2O_4$ are considered insoluble in water and the Hg(I) oxalate is only slightly soluble in dilute nitric acid.[27] Cleaning the filter with nitric acid may be the only option to remove deposited Hg.

5.0 Recommendations for Future Work

The following recommendations are made based upon items learned from this study:

1. Examine the primary filter now that we have examined three secondary filters to see if fines are also lodged in the filter media. This would include examining the primary filter for pockets of Hg.
2. Examine the filter performance of an entire filter tube from an existing secondary filter bundle to evaluate its performance and correlate this performance with the characterization data found for that filter.

3. Future filter examinations should look at larger pieces of filter than was done in this study where some pieces were as small as one quarter of a square inch. It is unclear what impact the intense localized heating created by the cutting tool had on these very small coupons as compared to larger coupons, but larger coupons would minimize this impact.
4. Leaching tests could be conducted on larger 3”L pieces of tube, while SEM could be conducted on 3”L tubes that were bisected into two halves and XRD/XRF measurements on halves that had been further size reduced by snapping rather than cutting.
5. To eliminate cross contamination, the Shielded Cells manipulator fingers and/or vice should be replaced prior to handling the samples, and kept clean between handling operations.

6.0 References

1 . Peters, T. B, Restivo, M. L., *512-S Secondary Filters Plugging Preliminary Analytical Analysis Summary and Status*, SRNL-L3100-2014-00252, Savannah River National Laboratory, Aiken, SC 29808 (October 2014).

2. Smith, S. P., *Analysis of 512-S Secondary Filters*, X-TTR-S-00019, Rev. 0, Savannah River Site, Aiken, SC 29808 (May 2014).

3. Restivo, M. L., Peters, T. B., *Task Technical and Quality Assurance Plan for Analysis of the 512-S Secondary Filters*, SRNL-RP-2014-00506, Savannah River National Laboratory, Aiken, SC 29808 (July 2014).

4. Restivo, M. L., "512-S Secondary Filter Plugging Analysis – Part 1A", Experiment O9117-00066-03, SRNL E-Notebook (Production), Savannah River National Laboratory, Aiken, SC 29808 (September 2014).

5. Restivo, M. L., "512-S Secondary Filter Plugging Analysis – Part 1B", Experiment O9117-00066-04, SRNL E-Notebook (Production), Savannah River National Laboratory, Aiken, SC 29808 (November 2014).

6. Bannochie, C. J., "512-S Secondary Filter Plugging Analysis – Part 2", Experiment L2320-00016-29, SRNL E-Notebook (Production), Savannah River National Laboratory, Aiken, SC 29808 (October 2014).

7. Peters, T. B., Fondeur, F. F., Fink, S. D., *Results from Analysis of Actinide Removal Process Guard Filter*, SRNL-STI-2009-00456, Rev. 1, Savannah River National Laboratory, Aiken, SC 29808 (January 2010).

8. *Integrated Data Base Report – 1984: U.S. Spent Nuclear Fuel and Radioactive Waste Inventories, Projections, and Characteristics*, DOE/RW-0006, Rev. 11, Oak Ridge National Laboratory, Oak Ridge, TN (September 1995).

9. Bannochie, C. J., "512-S Secondary Filter Plugging Analysis – Part 3", Experiment L2320-00016-30, SRNL E-Notebook (Production), Savannah River National Laboratory, Aiken, SC 29808 (October 2014).

10. Bannochie, C. J., "512-S Secondary Filter Plugging Analysis – Part 4", Experiment L2320-00016-31, SRNL E-Notebook (Production), Savannah River National Laboratory, Aiken, SC 29808 (October 2014).

11. Bannochie, C. J., "512-S Secondary Filter Plugging Analysis – Part 5", Experiment L2320-00016-32, SRNL E-Notebook (Production), Savannah River National Laboratory, Aiken, SC 29808 (November 2014).

12. Bannochie, C. J., "512-S Secondary Filter Plugging Analysis – Part 6", Experiment L2320-00016-33, SRNL E-Notebook (Production), Savannah River National Laboratory, Aiken, SC 29808 (November 2014).

13. Bannochie, C. J., "512-S Secondary Filter Plugging Analysis – Part 7", Experiment L2320-00016-34, SRNL E-Notebook (Production), Savannah River National Laboratory, Aiken, SC 29808 (November 2014).

14. Bannochie, C. J., "512-S Secondary Filter Plugging Analysis – Part 8", Experiment L2320-00016-35, SRNL E-Notebook (Production), Savannah River National Laboratory, Aiken, SC 29808 (November 2014).

15. Bannochie, C. J., "512-S Secondary Filter Plugging Analysis – Part 9", Experiment L2320-00016-36, SRNL E-Notebook (Production), Savannah River National Laboratory, Aiken, SC 29808 (November 2014).

16. Bannochie, C. J., "512-S Secondary Filter Plugging Analysis – Part 10", Experiment L2320-00016-37, SRNL E-Notebook (Production), Savannah River National Laboratory, Aiken, SC 29808 (November 2014).

17. Hobbs, D. T., "Properties and Uses of Sodium Titantates and Peroxotitanates", *J. SC Acad. Sci.*, **9**, 20-24 (2011).

18. Pike, J. A., Preliminary Evaluaton of Solids Precipitation in the ARP/LWHT with Sump Residue in Surge Tank, SRNL-L4220-2014-00010, Rev. 1, Savannah River National Laboratory, Aiken, SC 29808 (August 2014).

19. Campbell, S. E., *Blend Evaluation for Tank 49 Feed for ISDP Salt Batch 2*, X-ESR-H-00209, Savannah River Remediation, Aiken, SC 29808 (December 2008).

20. Campbell, S. E., *Blend Evaluation for Tank 49 Feed for ISDP Salt Batch 3*, X-ESR-H-00209, Savannah River Remediation, Aiken, SC 29808 (March 2010).

21. Campbell, S. E., *Blend Evaluation for Tank 49 Feed for ISDP Salt Batch 4*, X-ESR-H-00352, Savannah River Remediation, Aiken, SC 29808 (October 2011).

22. Campbell, S. E., *Blend Evaluation for Tank 49 Feed for ISDP Salt Batch 6-D*, X-ESR-H-00501, Savannah River Remediation, Aiken, SC 29808 (April 2013)

23. McWhorter, D. L., *Blend Evaluation for Tank 49 Feed for ISDP Salt Batch 7-B*, X-ESR-H-00691, Savannah River Remediation, Aiken, SC 29808 (July 2014).

24. Hobbs, D. T., *Concentrations of Metals and Non-Metals in Alkaline Waste Slurries*, WSRC-TR-96-0058, Savannah River Technology Center, Aiken, SC 29808 (April 1996).

25. *Solubilities of Inorganic and Metal-Organic Compounds*, 4th Ed., Vol. I and II, D. Van Nostrand Company, Inc. Princeton, NJ, 1958.

26. Bannochie, C. J., *Results for the Third Quarter 2013 Tank 50 WAC Slurry Sample*, SRNL-STI-2013-00651, Rev. 1, Savannah River National Laboratory, Aiken, SC 29808 (September 2014).

27. *CRC Handbook of Chemistry and Physics*, 95th Ed., Haynes, W. M., Lide, D. R., Ed.; CRC Press: Boca Raton, FL, 2014, Section 4, pp. 75-76.

Distribution:

S. L. Marra, 773-A
T. B. Brown, 773-A
D. H. McGuire, 999-W
S. D. Fink, 773-A
C. C. Herman, 773-A
E. N. Hoffman, 999-W
F. M. Pennebaker, 773-42A
W. R. Wilmarth, 773-A
Records Administration (EDWS)

J. M. Bricker, 704-30S
J. S. Contardi, 704-56H
T. L. Fellinger, 766-H
E. J. Freed, 704-S
J. M. Gillam, 766-H
B. A. Hamm, 766-H
E. W. Holtzscheiter, 766-H
J. F. Iaukea, 704-27S
D. K. Peeler, 999-W
J. W. Ray, 704-27S
P. J. Ryan, 210-S
M. A. Rios-Armstrong, 766-H
H. B. Shah, 766-H
D. C. Sherburne, 704-S
M. E. Stone, 999-W

T. B. Peters, 773-42A
M. L. Restivo, 773-42A
M. R. Poirier, 773-42A
D. T. Herman, 735-11A
C. J. Martino, 999-W

E. A. Brass, 241-12H
C. K. Chiu, 704-27S
E. J. Freed, 704-S
A. G. Garrison, 241-12H
B. A. Gifford, 704-56H
D. J. Martin, 241-152H
R. T. McNew, 241-152H
A. Samadi-Dezfouli, 704-27S
A. R. Shafer, 704-27S
T. E. Smith,241-52H

P. R. Jackson, DOE-SR, 703-46A
J. A. Crenshaw, 703-46A